Figure 1

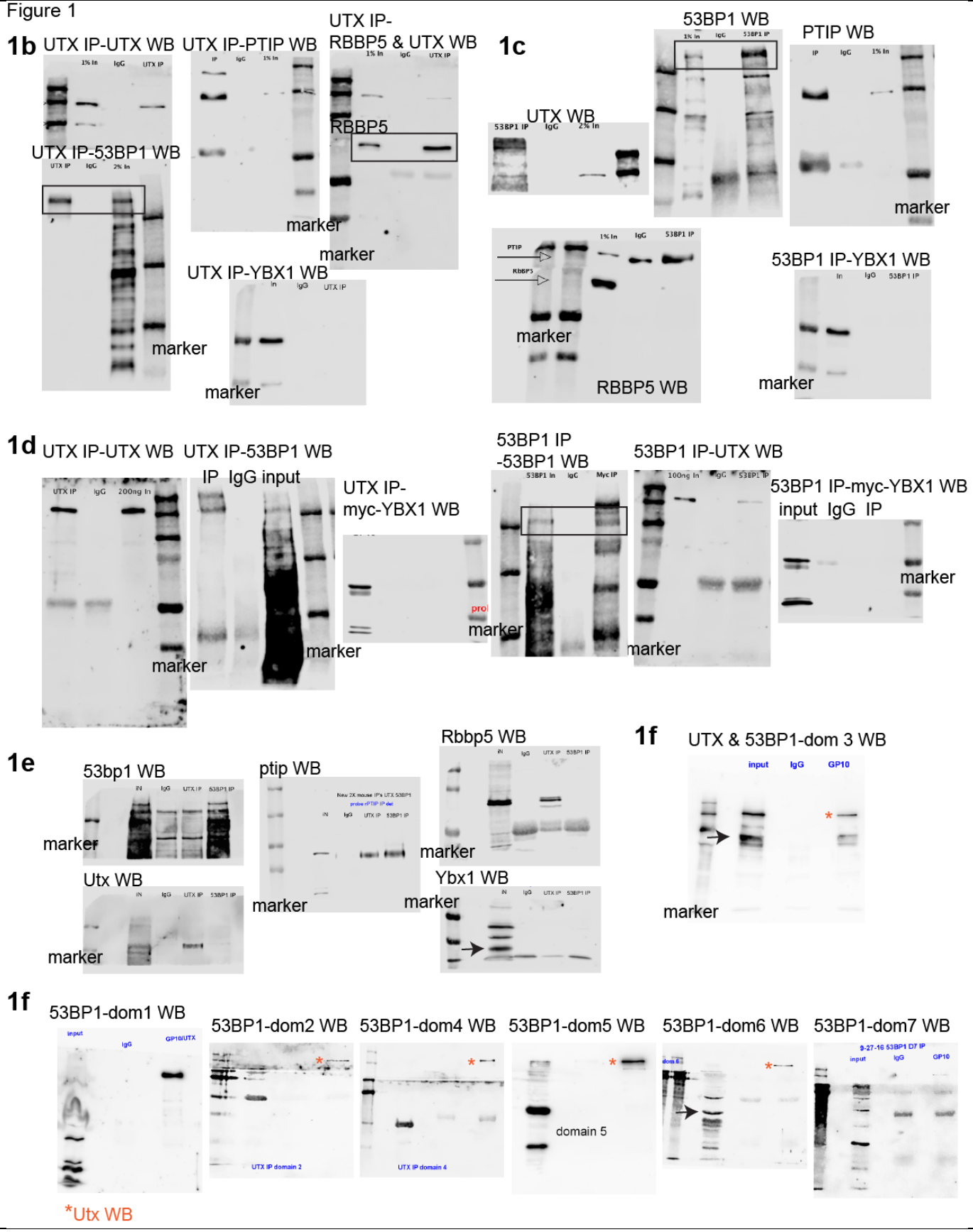
1b
UTX IP-UTX WB
UTX IP-PTIP WB
UTX IP-RBBP5 & UTX WB
UTX IP-53BP1 WB
RBBP5
marker
marker
marker
UTX IP-YBX1 WB
marker
1c
53BP1 WB
PTIP WB
UTX WB
marker
PTIP
RBBP5
marker
RBBP5 WB
53BP1 IP-YBX1 WB
marker
1d
UTX IP-UTX WB
UTX IP-53BP1 WB
IP IgG input
UTX IP-myc-YBX1 WB
53BP1 IP -53BP1 WB
53BP1 IP-UTX WB
53BP1 IP-myc-YBX1 WB
input IgG IP
marker
marker
marker
marker
marker
1e
53bp1 WB
ptip WB
Rbbp5 WB
marker
marker
marker
Utx WB
Ybx1 WB
marker
marker
1f
UTX & 53BP1-dom 3 WB
input IgG GP10
marker
1f
53BP1-dom1 WB
53BP1-dom2 WB
53BP1-dom4 WB
53BP1-dom5 WB
53BP1-dom6 WB
53BP1-dom7 WB
domain 5
*Utx WB

Figure 1 (cont'd)

Supp. Fig 2

1h h or m dom3 pull
myc-dom3 WB

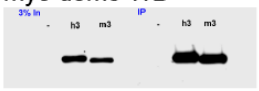

h or m dom3 pull
UTX WB

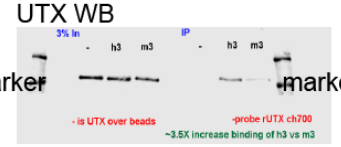

marker marker

1i h or m dom3iii pull
myc-dom3iii WB

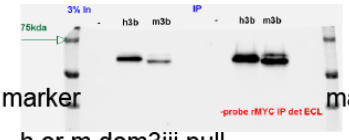

marker marker

h or m dom3iii pull
UTX WB

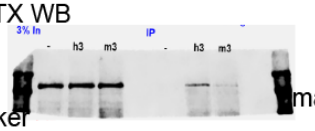

marker marker

S2b UTX WB

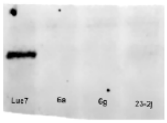

ACTB WB

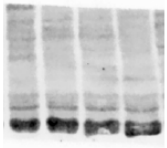

marker

S2e 53BP1-dom3 IP
53BP1-dom3 WB

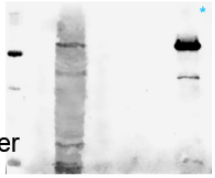

marker

53BP1-dom3 IP
UTX WB

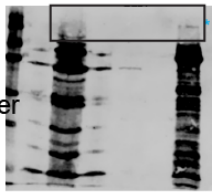

marker

S2f 53BP1-dom3i pull
53BP1-dom3i WB

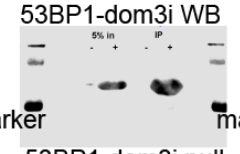

marker marker

53BP1-dom3ii & 3iii pull
dom WB

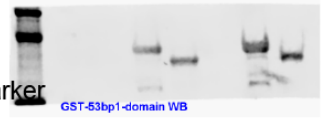

53BP1-dom3i pull
UTX WB

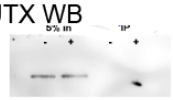

53BP1-dom3ii & 3iii pull
UTX WB

marker

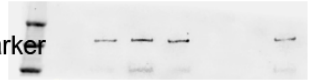

3b marker ctrl ko1 ko2 ko3

53BP1 WB

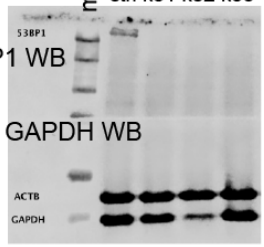

ACTB, GAPDH WB

UTX WB
ctrl1 ctrl2 ko1ko2ko3

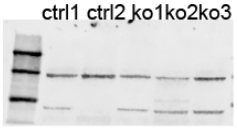

5b UTX WB
ctrl 1 2 3

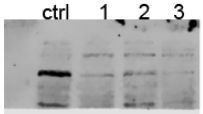

TUB, ACTB, GAPDH WB

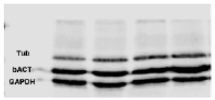

6b 53BP1 mut1

53BP1 WB

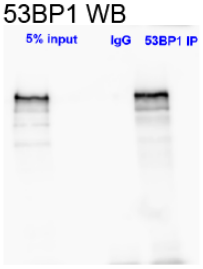

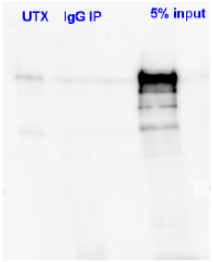

UTX WB

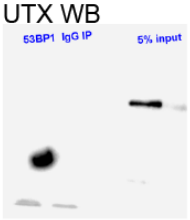

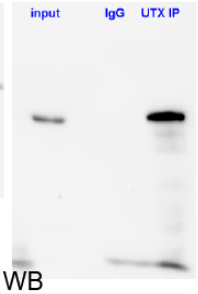

PTIP WB

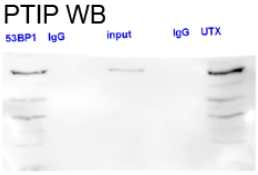

RBBP5 WB

YBX1 WB

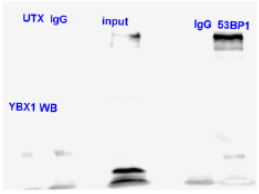

6b
53BP1 mut2

53BP1 WB

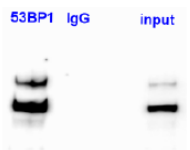

UTX WB

PTIP WB

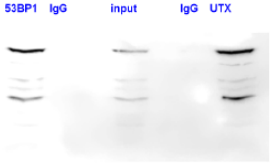

RBBP5 WB

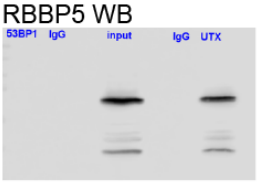

YBX1 WB

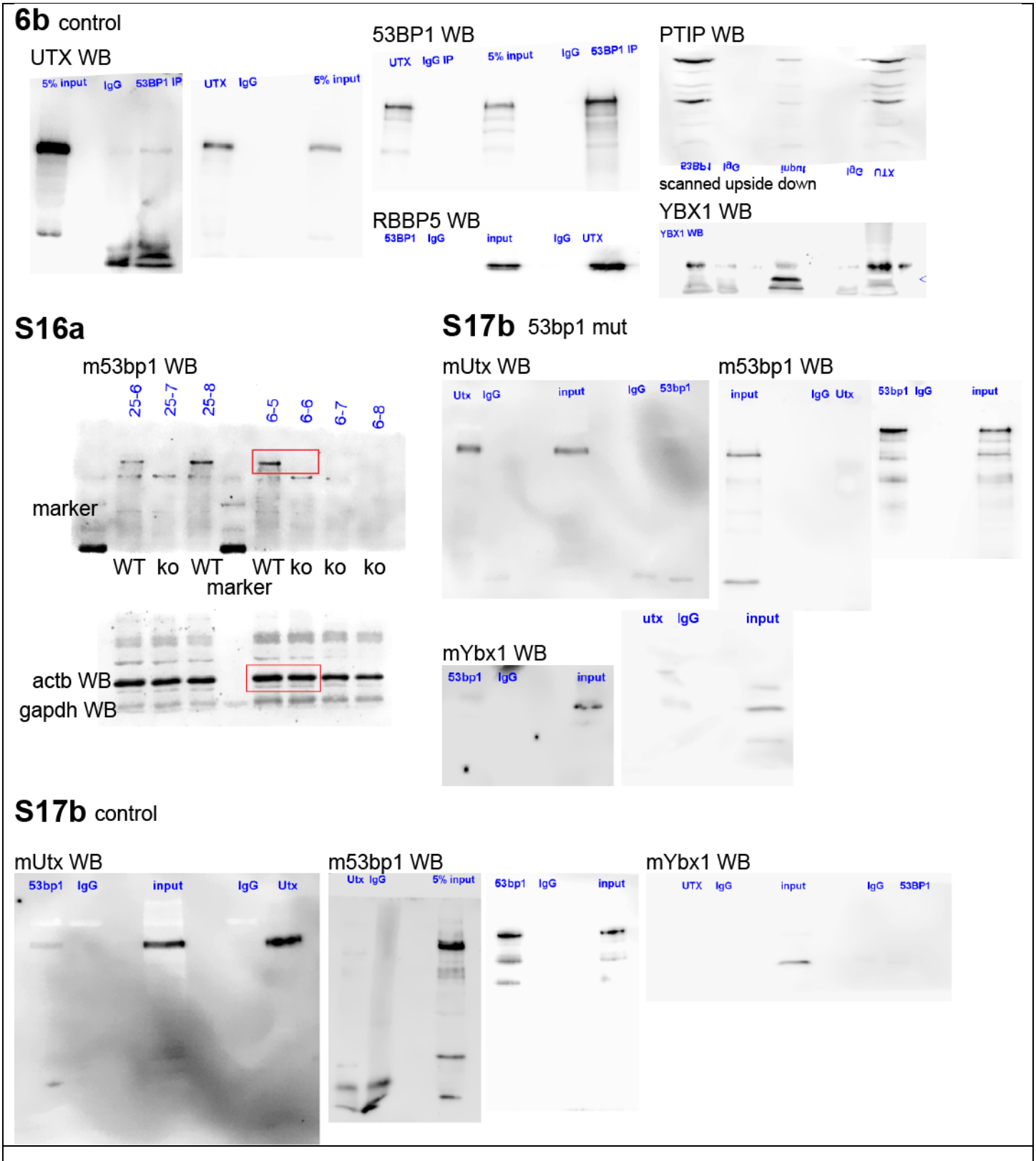

Supplementary Figure 1

Full scan of all western blots in this paper.

No caption.

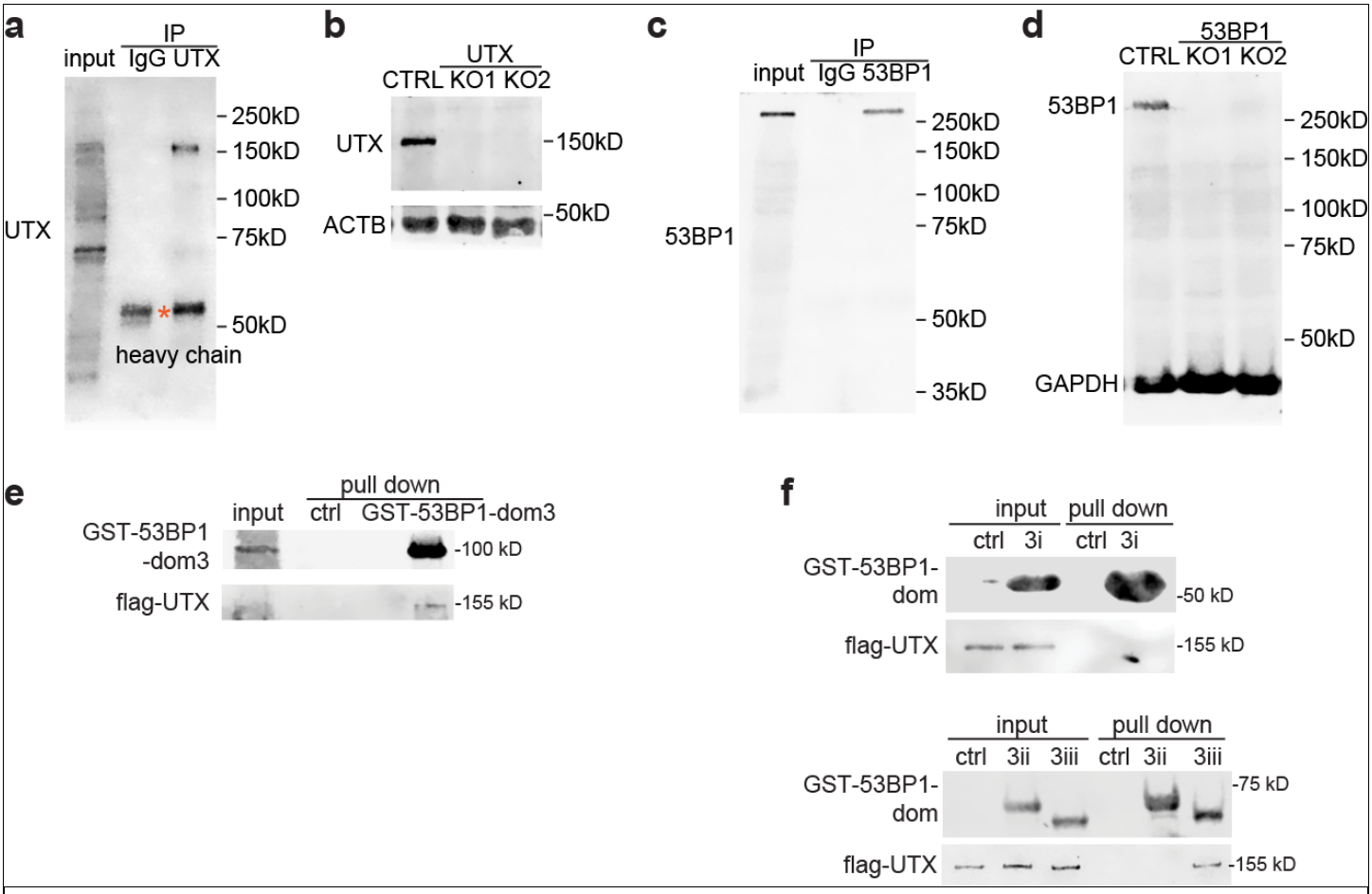

Supplementary Figure 2

WB analysis of immunoprecipitation and pull down.

WB analysis of (A) IgG and UTX IP; (B) control and UTX-KO nuclear extract; (C) IgG and 53BP1 IP; (D) control and 53BP1-KO nuclear extract; (E) glutathione IP of control and GST-tagged human 53BP1-domain 3; and (F) glutathione IP of control and GST-human 53BP1 domains 3i, 3ii, and 3iii with full-length flag-UTX. Experiments were repeated 2 times for a-d and 3 times for e-f to yield similar results. WB images are cropped.

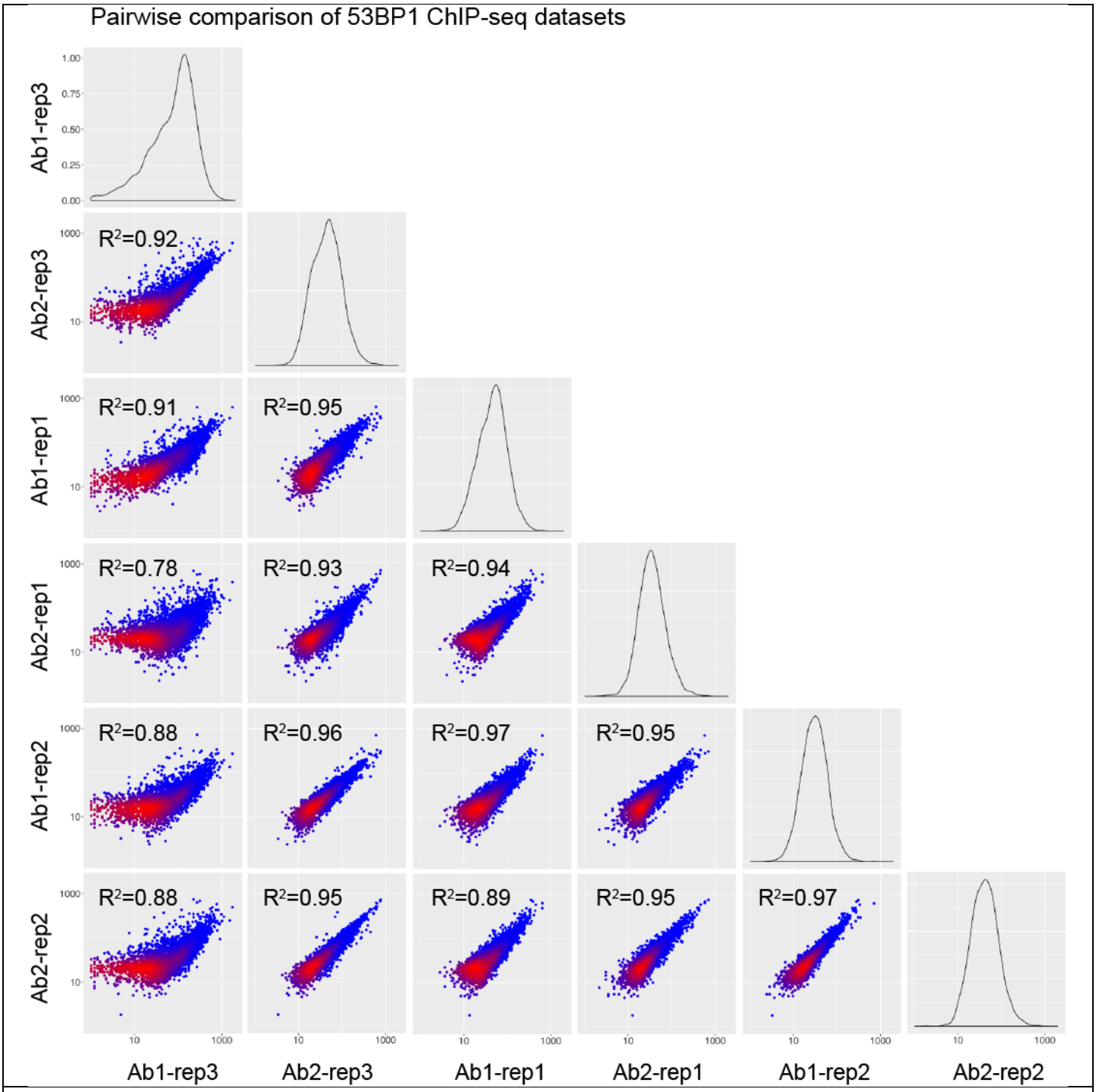

Supplementary Figure 3

High correlation between the 6 biological replicate datasets of 53BP1 ChIP-seq from 2 antibodies.

Each dataset is ChIP-seq signals at binned genomic regions. Pairwise counts per million of the datasets, with respective R^2 values are Pearson correlation coefficients. Red indicates a higher density of points. Diagonal curve plots show the kernel density of ChIP-seq reads in each dataset.

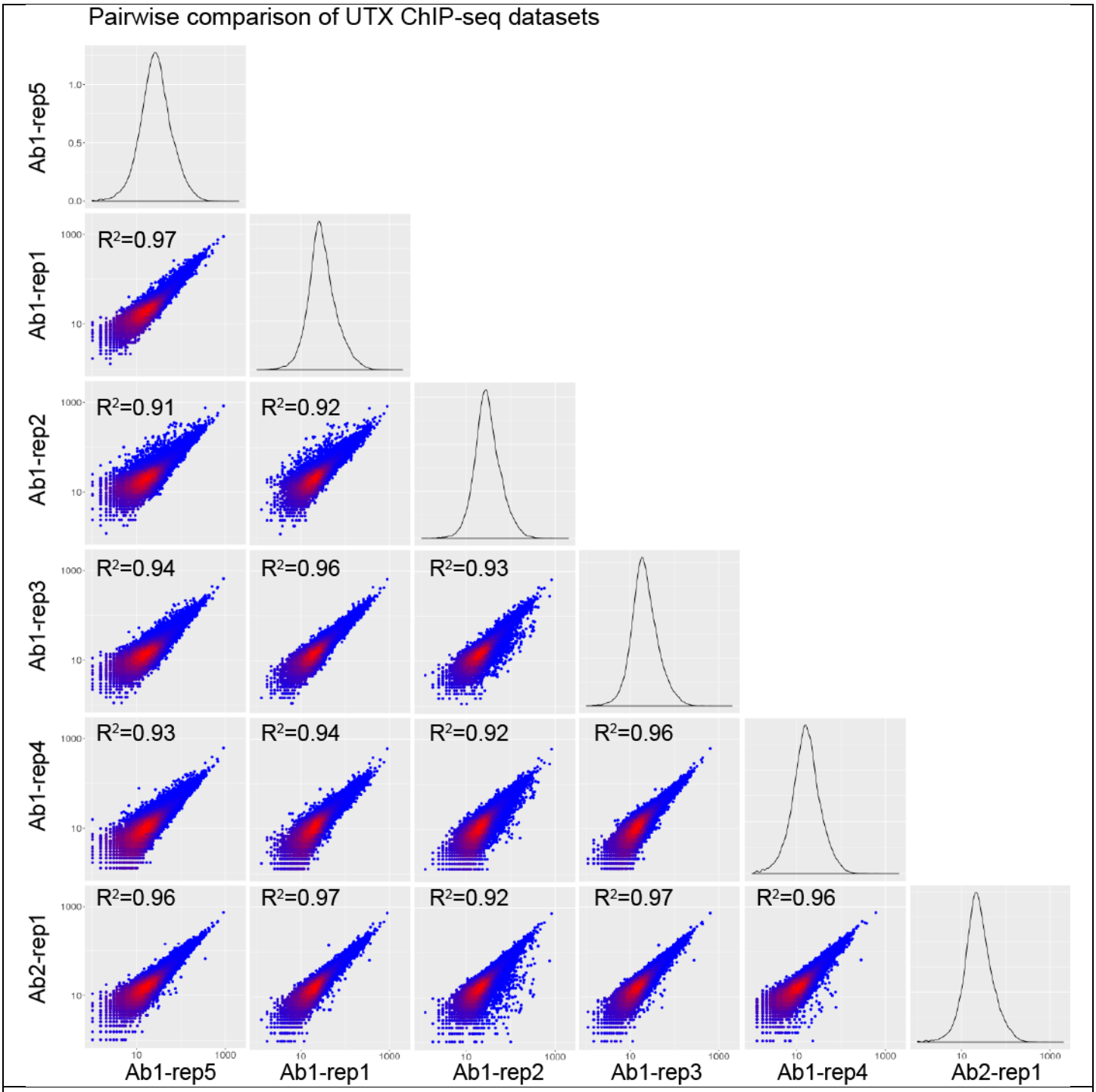

Supplementary Figure 4

High correlation between the six biological replicate datasets of UTX ChIP-seq from two antibodies.

Each dataset is ChIP-seq signals at binned genomic regions. Pair-wise counts per million of the datasets with respective R^2 values are Pearson correlation coefficients. Red indicated higher density of points. Diagonal curve plots show the kernel density of ChIP-seq reads in each dataset.

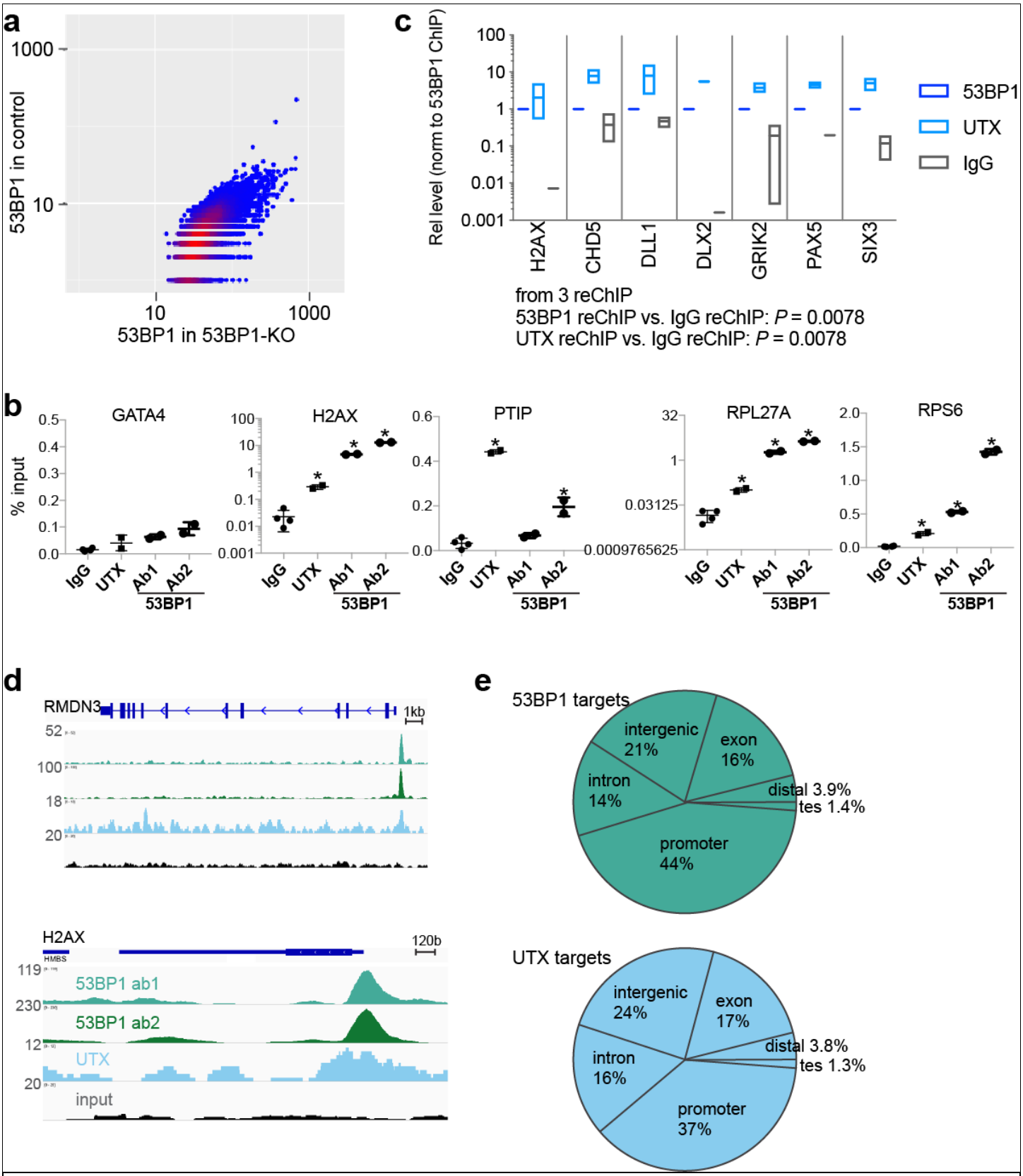

Supplementary Figure 5

UTX and 53BP1 bindings are enriched at transcription start sites.

(a) Low correlation between 53BP1 ChIP-seq in control and 53BP1-KO cells. Correlated was analyzed by using linear model of Goodness-of-Fit package in R. Each dataset contains ChIP-seq signals at binned genomic regions. The graph displays pairwise counts per million of the datasets, with Red indicating a higher density of points. 1 sample each was used in the analysis. (b) Validation of ChIP-seq targets of UTX and 53BP1 by ChIP-qPCR. The relative enrichment of H2AX, PTIP, RPL27A, and RPS6 promoters was quantified via IgG, UTX, and 53BP1 ChIP. The GATA4 promoter was the negative control. N=3 technical qPCR values; 2 biological repeats yielded similar results. Center values and error bars are mean and standard deviation. * indicates P <0.001 by one-sided Student's t test. (c) Summary data from 3 independent re-ChIP-qPCR experiments. For each experiment, the relative levels of UTX and IgG ChIP were normalized to 53BP1 re-ChIP. 53BP1 and UTX ChIP are significantly higher than IgG ChIP, using one-sided paired t test. N=3. Center values and error bars are mean and standard deviation. (d) Representative 53BP1 and UTX ChIP-seq tracks peak at the transcription start site of the RMDN3 or H2AX locus. The input DNA track is displayed for comparison. Experiments were repeated 6 times to yield similar results. (e) Pie charts indicate the proportions of UTX or 53BP1 binding site enrichment. 'Distal' indicates regions that are 5 kb from transcription start sites. 'Tes' denotes transcription termination sites.

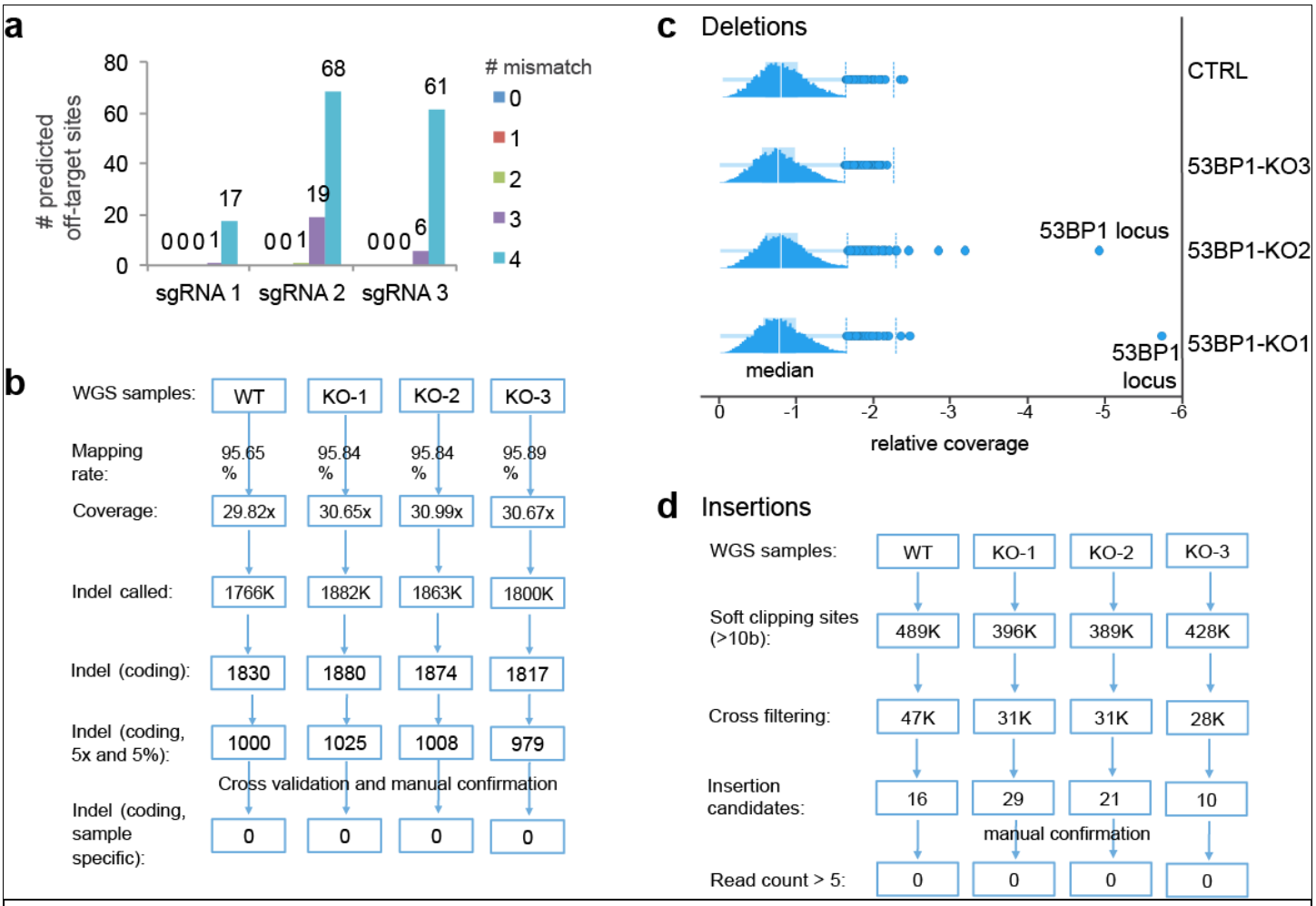

Supplementary Figure 6

Whole-genome sequencing analyses.

(a) Numbers of predicted off-target sites with 0-4 mismatches to each of three CRISPR gRNAs used in the study. (b) Summary flow chart of sequencing analysis to detect small insertions and deletions (indel). Against the human reference genome (hg19), detected indels were filtered by the listed criteria, removed while present in more than one sample or sample group, and manually confirmed excluding sequencing or mapping errors. A 7-bp deletion in KO-3, specific to the 53BP1-KO line, was the only functionally related indel detected through the workflow. (c) Deletion analysis. The relative coverage analysis among this group of samples, targeting for deletions larger than 50 bp, was performed to only identify two deletions within the 53BP1 locus of the 53BP1-KO cells. (d) Summary flow chart of insertion analysis. The soft-clipped reads (>10 bp overhang) were extracted and used to detect larger insertions that were failed to report in previous indel analysis. Soft-clipping break points were summarized as genomic locations, cross filtering between samples was to remove non-specific locations, and the potential insertion sites were defined as a pair of bi-direction break points within a 5-bp window. After removing the low coverage noise, the insertion event in KO-3, specific to the 53BP1-KO lines, was the only insertion reported through the workflow.

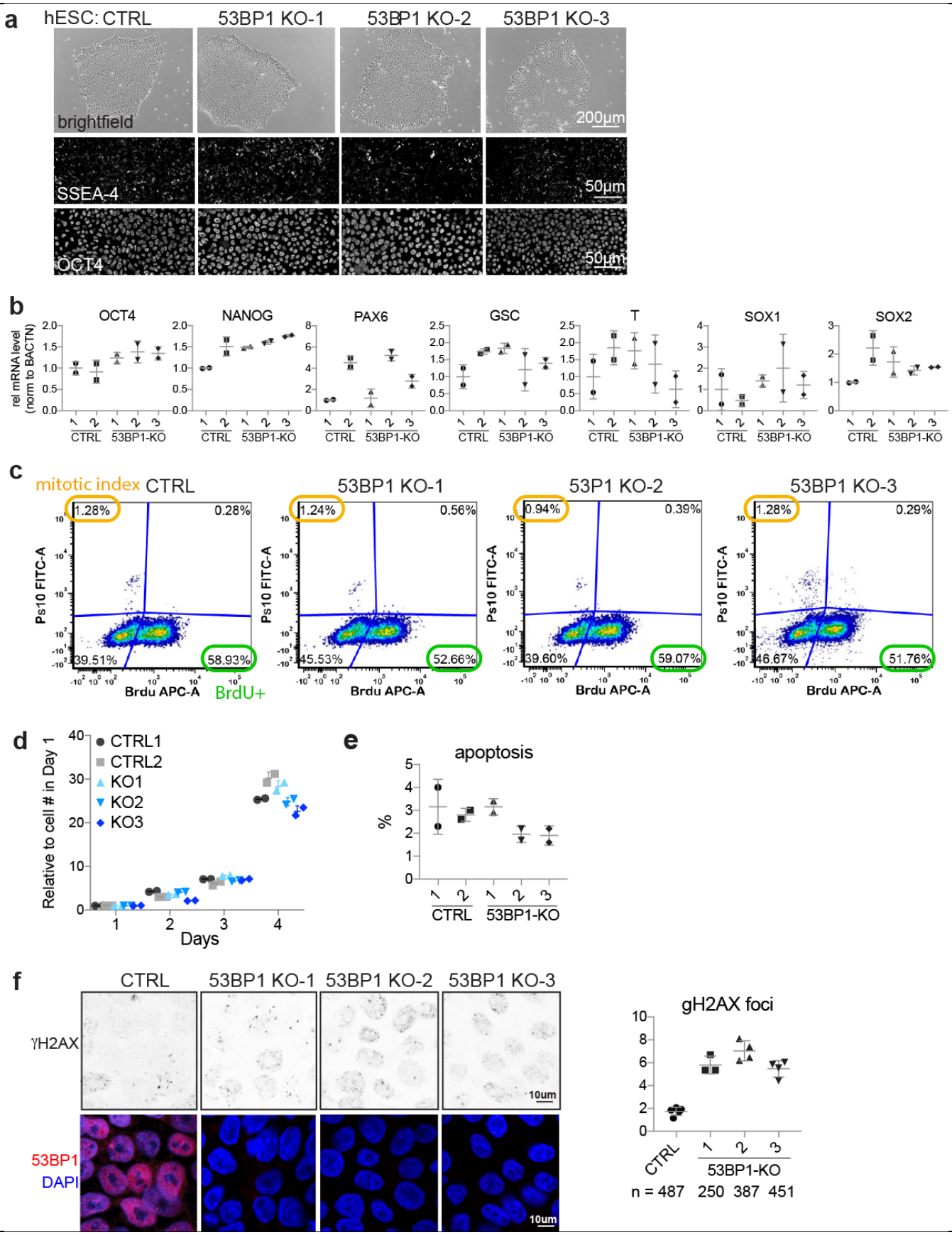
a
hESC: CTRL
53BP1 KO-1
53BP1 KO-2
53BP1 KO-3
brightfield
200μm
SSEA-4
50μm
OCT4
50μm
b
rel mRNA level (norm to BACTN)
OCT4
NANOG
PAX6
GSC
T
SOX1
SOX2
CTRL
53BP1-KO
c
mitotic index
CTRL
53BP1 KO-1
53P1 KO-2
53BP1 KO-3
Ps10 FITC-A
Brdu APC-A
BrdU+
1.28%
0.28%
39.51%
58.93%
1.24%
0.56%
45.53%
52.66%
0.94%
0.39%
39.60%
59.07%
1.28%
0.29%
46.67%
51.76%
d
Relative to cell # in Day 1
CTRL1
CTRL2
KO1
KO2
KO3
Days
e
apoptosis
%
CTRL
53BP1-KO
f
CTRL
53BP1 KO-1
53BP1 KO-2
53BP1 KO-3
γH2AX
53BP1
DAPI
10um
gH2AX foci
CTRL
53BP1-KO
n = 487 250 387 451

Supplementary Figure 7

53BP1 does not affect pluripotency, apoptosis, or proliferation of hESCs.

(a) Bright field imaging (Top), SSEA-4 immunofluorescence (IF) (Middle), and OCT4 IF (Bottom) of control cells and 53BP1 KO clones 1-3. (b) Quantification of relative expression of pluripotency markers or germ layer markers in 2 control and 3 53BP1-KO clones. Marker cDNA was quantified by performing RT-qPCR, with circles and bars indicating mean and standard deviation values, respectively. Control and 53BP1-KO cells did not differ significantly by the Student's *t* test. N=3 technical RT samples. Center values and error bars are mean and standard deviation. No statistical significance by one-sided t test. (c) The proportion of mitotic or BrdU-positive cells in control and 3 53BP1-KO clones was quantified by performing FACS of phosphorylated-serine 10 in histone H3 and BrdU labeling. (d) Relative cell numbers of 2 control and 3 53BP1-KO clones proliferating over 4 days. N=2 biological samples for each group. No significant difference by the chi-squared test. (e) The proportion of apoptotic cells in 2 control and 3 53BP1-KO clones. Apoptosis was quantified via annexin V and propidium iodide FACS. N=2 biological samples for each group. No significant difference by the chi-squared test. (f) γH2AX and 53BP1 IF analysis of control cells and 53BP1 KO clones 1-3. For ease of visualization, the high intensity of the γH2AX IF signal is black. Bars, 10 μm. N=487, 250, 387, and 451 cells. Graph at right summarizes foci quantification, with center values and error bars being mean and standard deviation, and **** P <0.0001 by the ANOVA test.

a

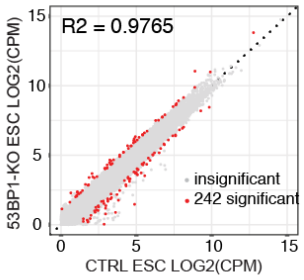

c

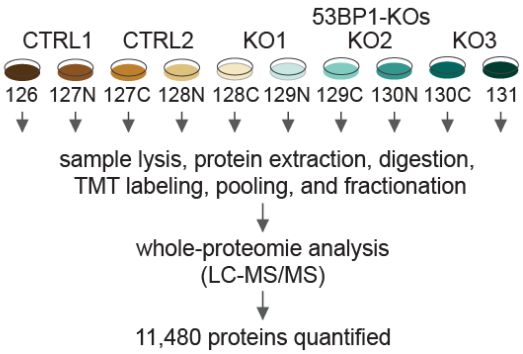

b

53BP1-bound genes, 675 downregulated in 53BP1 KO hESC	# Genes	*P* value
positive regulation of transcription from RNA polymerase II promoter	83	3.32E-13
cell-cell adhesion	36	4.05E-11
transcription, DNA-templated	114	9.88E-08
regulation of mRNA stability	17	6.95E-07
negative regulation of transcription from RNA polymerase II promoter	51	5.06E-06
actin cytoskeleton organization	16	6.07E-05
negative regulation of epidermal growth factor receptor signaling pathway	8	2.38E-04
protein polyubiquitination	18	3.19E-04
Wnt signaling pathway	18	3.85E-04

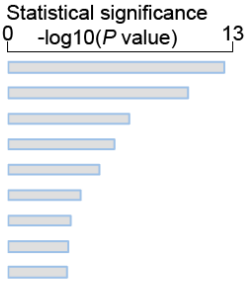

53BP1-bound genes, 886 upregulated in 53BP1 KO hESC	# Genes	*P* value
ER-associated ubiquitin-dependent protein catabolic process	17	3.52E-09
protein N-linked glycosylation	13	5.60E-08
membrane protein ectodomain proteolysis	9	2.31E-06
Notch receptor processing	8	2.33E-06
protein folding in endoplasmic reticulum	7	8.80E-06
dolichol-linked oligosaccharide biosynthetic process	7	2.38E-05
IRE1-mediated unfolded protein response	12	4.09E-05

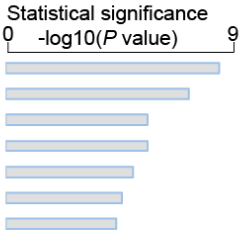

d

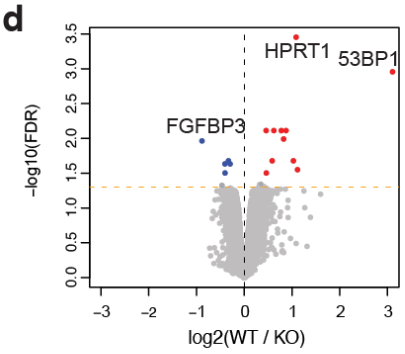

e

name	full name	protein accession #	peptide spectral match	KO / WT ratio
Downregulated in 53BP1-KO				
TP53BP1	Tumor suppressor p53-binding protein 1	sp|Q12888|TP53B_HUMAN	115	0.09
SP140L	Nuclear body protein SP140-like protein	sp|Q9H930|SP14L_HUMAN	1	0.37
MT1G	Metallothionein-1G	sp|P13640|MT1G_HUMAN	10	0.39
S100A13	Protein S100-A13	sp|Q99584|S10AD_HUMAN	14	0.40
GSDMD	Gasdermin-D	sp|P57764|GSDMD_HUMAN	9	0.44
CAMK2A	Calcium/calmodulin-dependent kinase type II alpha	tr|D6RFJ0|D6RFJ0_HUMAN	1	0.45
CCDC152	Coiled-coil domain-containing protein 152	sp|Q4G0S7|CC152_HUMAN	5	0.45
HPRT1	Hypoxanthine-guanine phosphoribosyltransferase	sp|P00492|HPRT_HUMAN	77	0.45
FOSL1	Fos-related antigen 1	sp|P15407|FOSL1_HUMAN	1	0.46
ZNF212	Zinc finger protein 212	sp|Q9UDV6|ZN212_HUMAN	7	0.52
ZNF638	Zinc finger protein 638	tr|A0A096LNQ0|A0A096LNQ0_HUMAN	68	0.53
TIMM50	Mitochondrial import inner membrane translocase subunit 50	tr|M0R303|M0R303_HUMAN	4	0.60
Upregulated in 53BP1-KO				
ACOT1	Acyl-coenzyme A thioesterase 11	sp|Q8WXI4|ACO11_HUMAN	29	1.36
ITGAE	Integrin alpha-E	sp|P38570|ITAE_HUMAN	2	1.49
PDE11A	Dual 3',5'-cyclic-AMP and -GMP phosphodiesterase 11A	sp|Q9HCR9|PDE11_HUMAN	1	1.65
FGFBP3	Fibroblast growth factor-binding protein 3	sp|Q8TAT2|FGFP3_HUMAN	15	1.85
RBM39	RNA-binding protein 39	tr|H0Y6I9|H0Y6I9_HUMAN	2	1.38

Supplementary Figure 8

Profiling of control and 53BP1-KO hESCs.

(a) Comparison of transcript profiles of 3 (biologically independent) 53BP1-KO, and 5 (biologically independent) control hESCs by counts per million of sequencing reads for each annotated gene. Correlation coefficients are calculated by using linear model of Goodness-of-Fit package in R. (b) Gene ontology analysis of differentially expressed genes in 4 53BP1-KO clones as compared to 3 control clones. Ontology terms were ranked by *P* values (by Fisher's exact test), with the number of differentially expressed genes indicated. (c) Duplicate samples of 2 control and 3 53BP1-KO hESCs were labeled were perspective tandem mass tags and subjected to quantitative mass spectrometry analysis. (d) Comparison of proteomic profiles of 3 53BP1-KO and 2 control hESCs by mass tag signals for each quantifiable protein. 2 biological replicates from each group were analyzed by the limma package, which powers differential expression analyses. (e) Summary table of 17 proteins whose levels significantly differed (using the Limma package [33]) between 53BP1-KO and control hESCs in at least 2 pairwise comparisons.

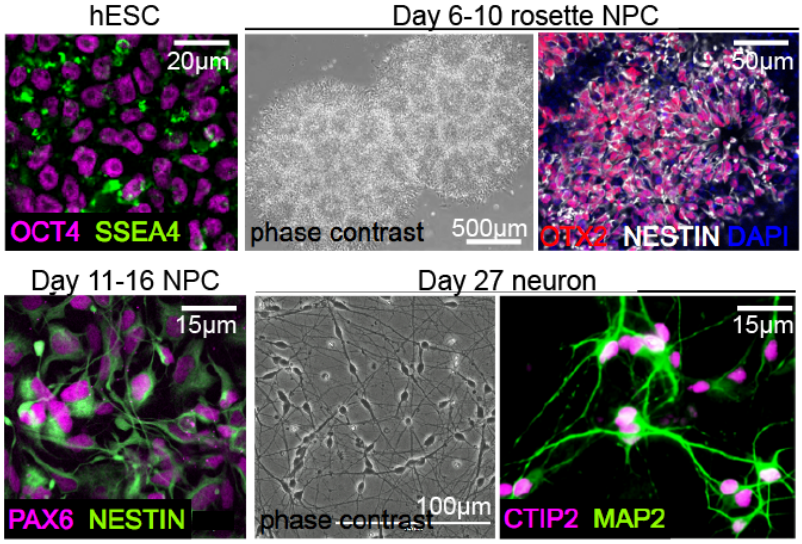

c

RNA-seq of hNPC, day 12 of differentiation

Enrichr human gene atlas	
Fetal brain	*P* value 5.26E-05

b upregulated in hNPC

Gene Ontology Term	# Genes	*P* value
nervous system development	75	6.09E-23
axon guidance	51	6.68E-20
anterior/posterior pattern specification	29	5.32E-13
positive regulation of synapse assembly	24	1.59E-11
positive regulation of transcription from RNA polymerase II	128	3.12E-11
negative regulation of transcription from RNA polymerase II	101	9.60E-11
neuron migration	30	1.55E-10
synapse assembly	21	4.15E-09
central nervous system development	30	4.67E-09
cell fate determination	12	4.99E-09

Supplementary Figure 9

Characterization of hNPCs.

(a) Bright field and IF imaging of cells at stages of the neural differentiation course. OCT4 and SSEA4 are markers for hESCs; OTX2, NESTIN, and PAX6, for hNPCs; and CTIP2 and MAP2, for mature cortical neurons. Experimetns were repeated 5 times to yield similar results. (b) Upregulated genes in hNPCs (Day 12 of neural lineage differentiation) that are enriched in terms related to nervous system development. (c) Analysis by Enrichr (http://amp.pharm.mssm.edu/Enrichr/) shows that the upregulated genes were enriched for the signature of human fetal brain. For b and c, the Fisher's exact test was used to calculate the *P* values.

a

53BP1 target genes

Gene ontology terms	# Genes	*P* value
hESC only		
DNA strand renaturation	12	3.40E-03
intraciliary anterograde transport	7	1.94E-03
DNA protection	11	5.47E-03
regulation of G2/M transition	8	6.93E-03
NAD biosynthesis via nicotinamide riboside salvage pathway	9	9.86E-03
DNA replication, synthesis of RNA primer	15	5.93E-03
both hESC and hNPC		
nuclear-transcribed mRNA catabolic process, 3'-5' exonucleolytic nonsense-mediated decay	123	2.04E-27
spliceosomal snRNP assembly	173	4.30E-19
late viral transcription	97	2.24E-22
mRNA splicing, via spliceosome	176	6.71E-19
hNPC only		
axon guidance	30	1.92E-03
commissural neuron axon guidance	24	1.10E-03
retinal ganglion cell axon guidance	24	1.10E-03
sensory neuron axon guidance	23	2.00E-03
sympathetic neuron axon guidance	23	2.00E-03
axon choice point recognition	23	2.00E-03

b

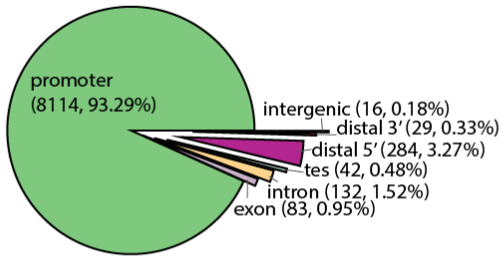

c

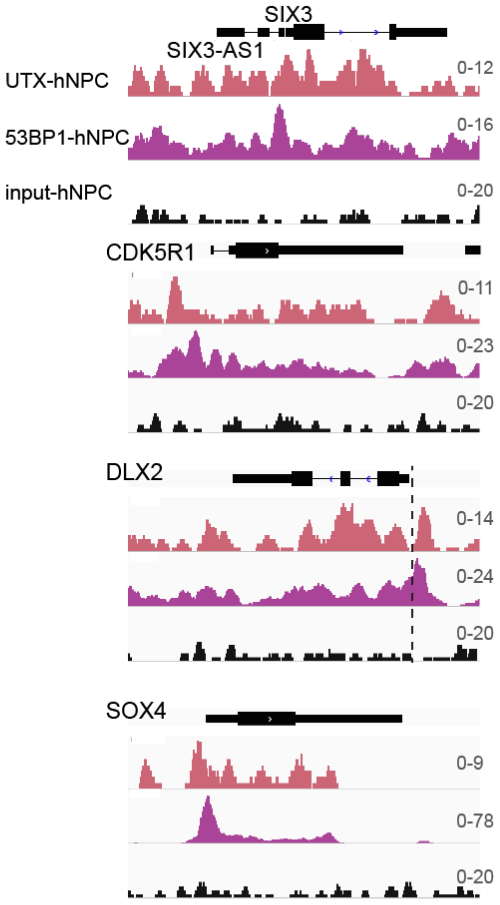

d

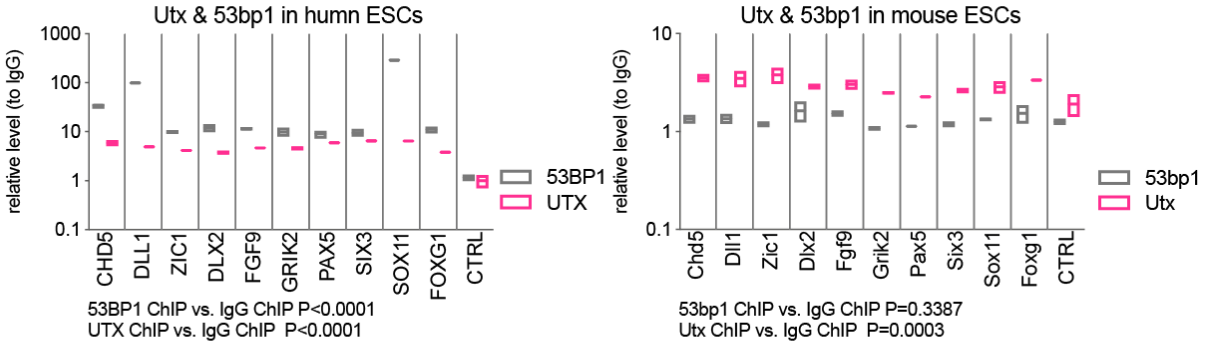

e

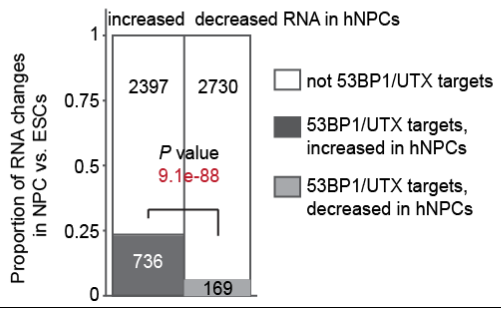

Supplementary Figure 10

53BP1 binding correlates with the activation of neurogenic genes in hNPCs.

(a) Gene ontology analysis of 53BP1 target genes. The ontology terms were ranked by *P* values (by the Fisher's exact test), with the number of bound genes indicated. (b) Pie charts indicate the proportions of UTX and 53BP1 enrichment. 'Distal' indicates regions that are 5 kb from transcription start sites. 'Tes' denotes transcription termination sites. (c) Representative 53BP1 and UTX ChIPseq tracks, with input track as negative control, at the gene locus of *SIX3, CDK5R1, DLX2,* and *SOX4* in hNPCs. Experiments were repeated 2 times to yield similar results. (d) ChIP-qPCR analysis of UTX and 53BP1 binding to the promoters of neurogenic genes in human and mouse ESCs. N=3 qPCR results; from 2 biologically independent experiments. Center values and error bars are mean and standard deviation. * and ** indicate $P<0.05$ and $P<0.001$ by one-sided Student's *t*-test. (e) Differentially expressed genes in hNPCs vs. hESCs were correlated to 53BP1 and UTX targets in hNPCs. The comparison of the 735 target genes that are upregulated/increased in hNPCs to the 169 target genes that are downregulated/decreased in hNPCs yielded $P= 9.1\times10^{-88}$ by the Fisher's exact test.

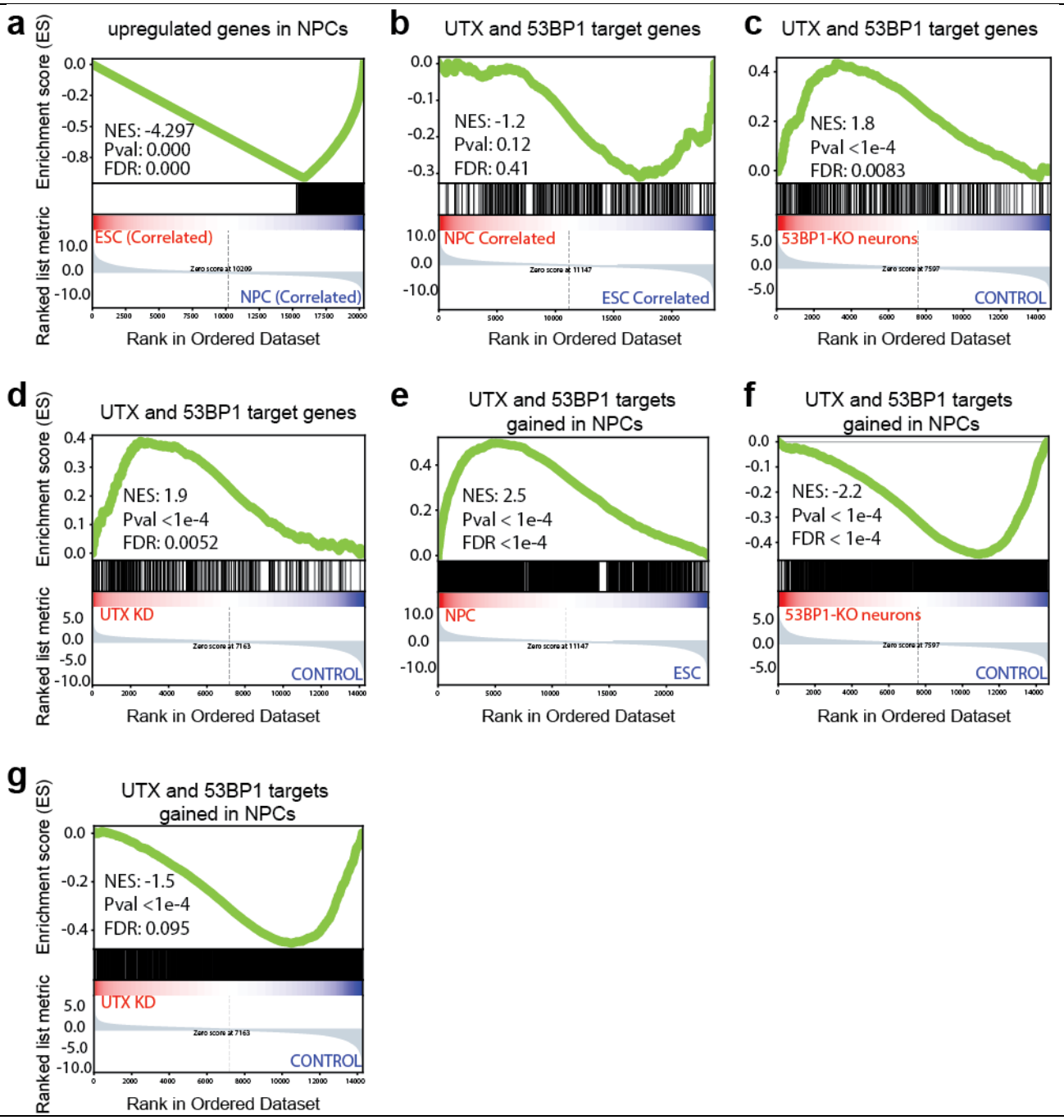

Supplementary Figure 11

Gene set enrichment analyses of UTX and 53BP1 targets in hESCs or target genes gained in hNPCs.

(a) Enrichment test of upregulated genes in hNPCs (vs. hESCs) with upregulated genes in hESCs (vs. hNPCs) yielded strong negative correlation. Enrichment test of all UTX and 53BP1 target genes in hESCs with (b) differentially expressed genes in hNPCs (vs. hESCs) yielded no significance, (c) differentially expressed genes in 53BP1-KO mutant vs. control yielded significant positive correlation, and (d) differentially expressed genes in UTX mutant vs. control yielded significant positive correlation. Enrichment test of UTX and 53BP1 target genes gained during hNPC differentiation with (e) differentially expressed genes in hNPCs (vs. hESCs) yielded strong positive correlation, (f) differentially expressed genes in 53BP1-KO mutant vs. control yielded significant negative correlation, and (g) differentially expressed genes in UTX mutant vs. control significant negative correlation. For all GSEA, ChIP were 6 biological samples in hESCs and 2 biological samples in hNPCs, and *P* values are nominal P values.

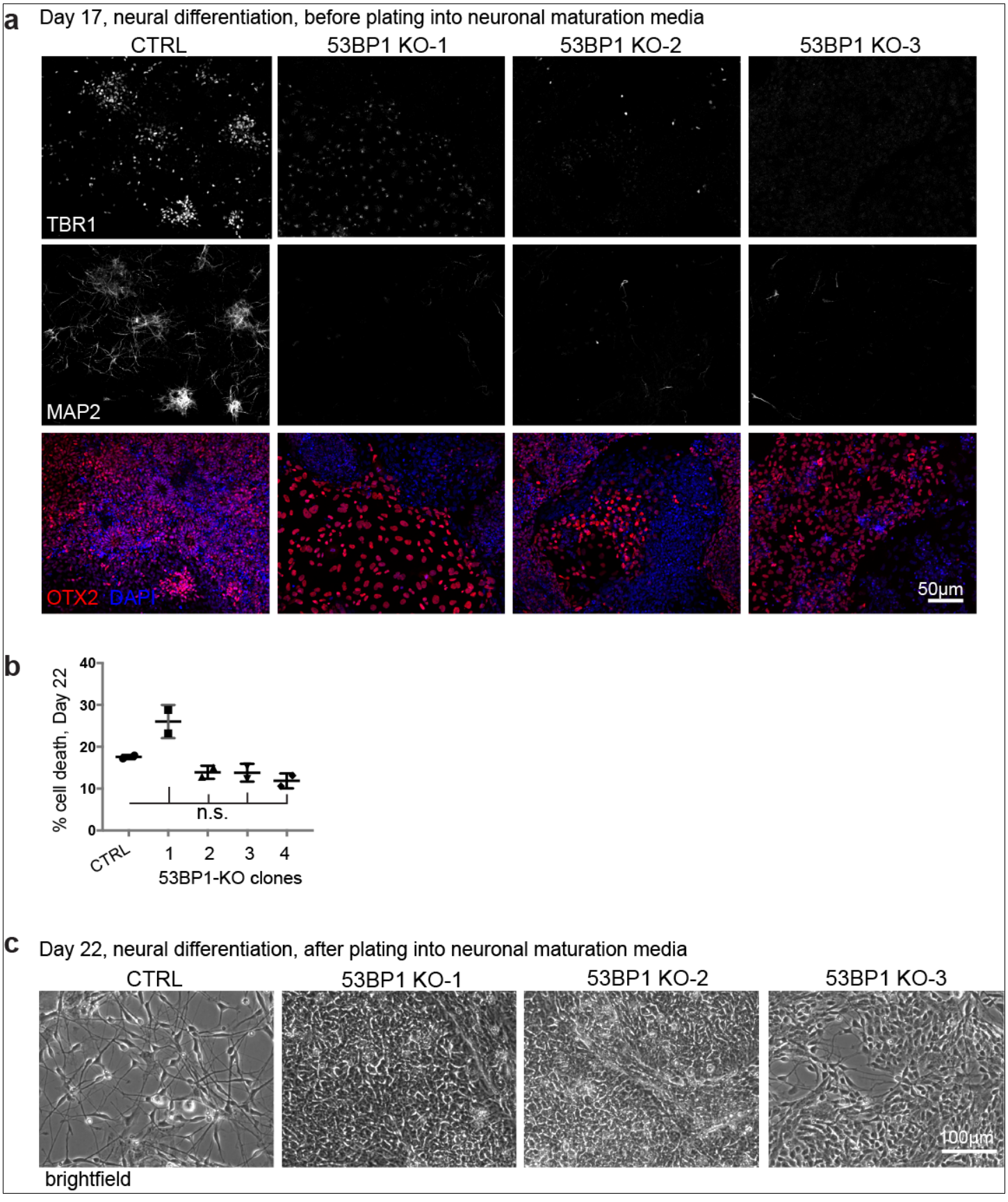
a
Day 17, neural differentiation, before plating into neuronal maturation media
CTRL
53BP1 KO-1
53BP1 KO-2
53BP1 KO-3
TBR1
MAP2
OTX2 DAPI
50µm
b
% cell death, Day 22
40
30
20
10
0
n.s.
CTRL
1
2
3
4
53BP1-KO clones
c
Day 22, neural differentiation, after plating into neuronal maturation media
CTRL
53BP1 KO-1
53BP1 KO-2
53BP1 KO-3
100µm
brightfield

Supplementary Figure 12

Compared to control cells, 53BP1-KO hNPCs failed to commit to neuronal differentiation.

(a) TBR1, MAP2, and OTX2 IF of control and 53BP1-KO hNPCs at day 17 of the neural lineage differentiation. Bar, 100μm. Cells were analyzed before being plated into neuronal maturation media. (b) Percentages of apoptotic cells determined via annexin v and propidium iodide FACS in control and 4 53BP1-KO cells at day 22 of differentiation. N=2 biological samples. n.s., not significant by one-sided Student's *t*-test. (c) Bright-field imaging of control and 53BP1-KO hNPCs at day 22 of differentiation, after 5 days in neuronal maturation media. Cells were plated at the same density at day 17. Because control cells have stopped dividing 3 days prior, their density was much sparser than those of 53BP1-KO cells. Experiments were repeated 3 times to yield similar results.

a

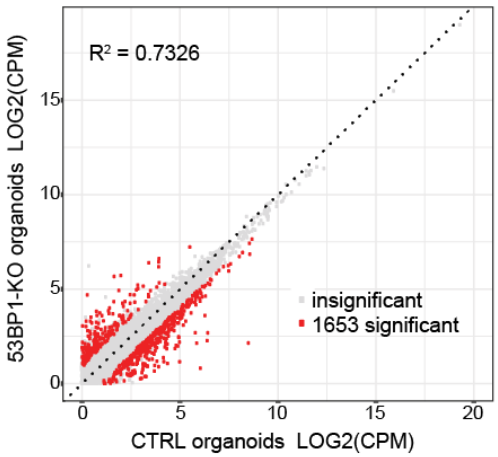

c Upregulated in 53BP1-KO cortical organoids

Term	Overlap	P-value
collagen fibril organization	25/154	1.84E-07
extracellular matrix disassembly	27/198	2.13E-06
biofilm matrix organization	22/143	2.50E-06
cellulose microfibril organization	22/143	2.50E-06
extracellular matrix organization	22/143	2.50E-06
fibronectin fibril organization	22/144	2.81E-06
extracellular matrix organization involved in endocardium development	22/143	2.50E-06
basement membrane organization	22/144	2.81E-06
gene expression involved in extracellular matrix organization	22/146	3.55E-06
extracellular matrix assembly	22/149	4.99E-06

b Downregulated in 53BP1-KO cortical organoids

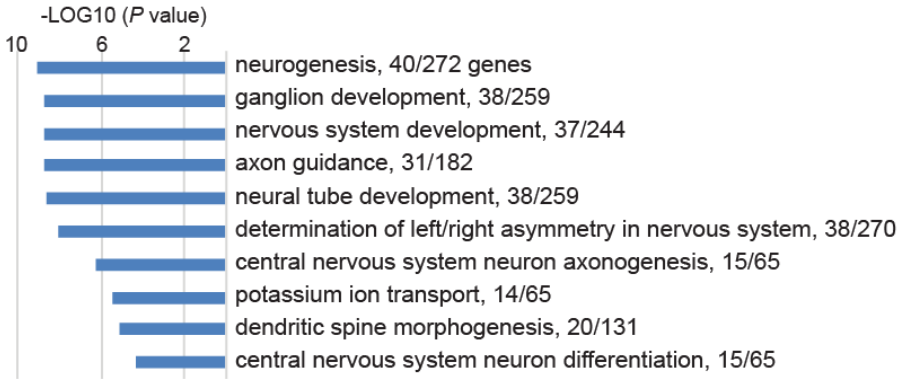

d

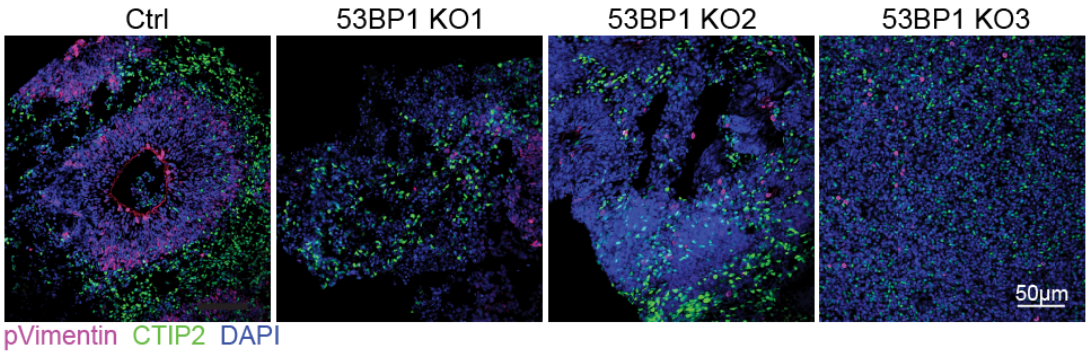

e

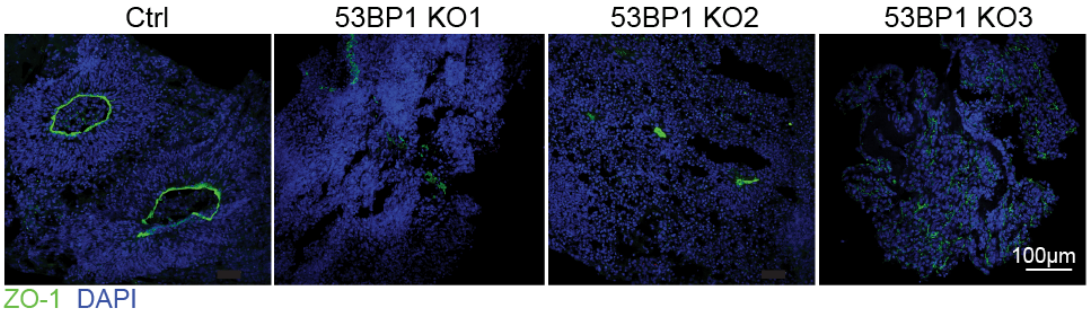

Supplementary Figure 13

53BP1 promotes neurogenic gene expression and development of cortical organoids.

(a) Comparison of transcript profiles of 53BP1-KO and control organoids by counts per million of sequencing reads for each annotated gene by using the modified t test from voom package in R. Two biological samples each from control, 53BP1-KO1, and 53BP1-KO2 were analyzed. Enriched terms of (b) downregulated genes and (c) upregulated genes in 53BP1-KO cortical organoids (vs. control); *P* values by the Fisher's exact test. Immunofluorescence of (d) phosphorylated-VIMENTIN and CTIP2, and (e) ZO-1, of sections from organoids at day 45 of differentiation. Bar, 50 μm. Experiments were repeated 2 times for d and e to yield similar results.

a

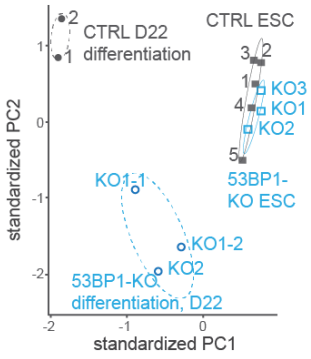

b Downregulated in 53BP1-KO, D22

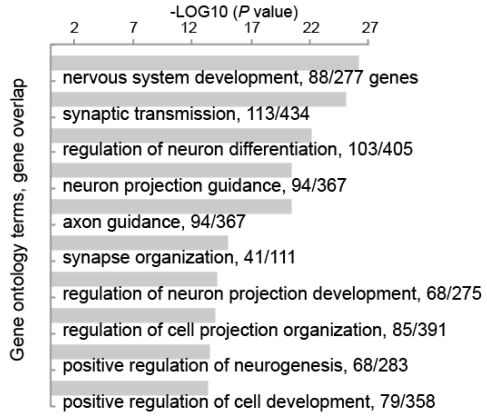

c

Upregulated in 53BP1-KO, Day 22	# Genes	*P* value
translational termination	40	2.08E-22
translational initiation	47	7.75E-20
nuclear-transcribed mRNA catabolic process, nonsense-mediated decay	43	7.39E-20
cellular protein complex disassembly	41	9.25E-19
SRP-dependent cotranslational protein targeting to membrane	40	1.04E-18
translational elongation	41	1.34E-18
establishment of protein localization to ER	41	1.94E-18
protein targeting to ER	40	3.26E-18
protein complex disassembly	43	1.42E-17
nuclear-transcribed mRNA catabolic process	47	1.40E-14

d

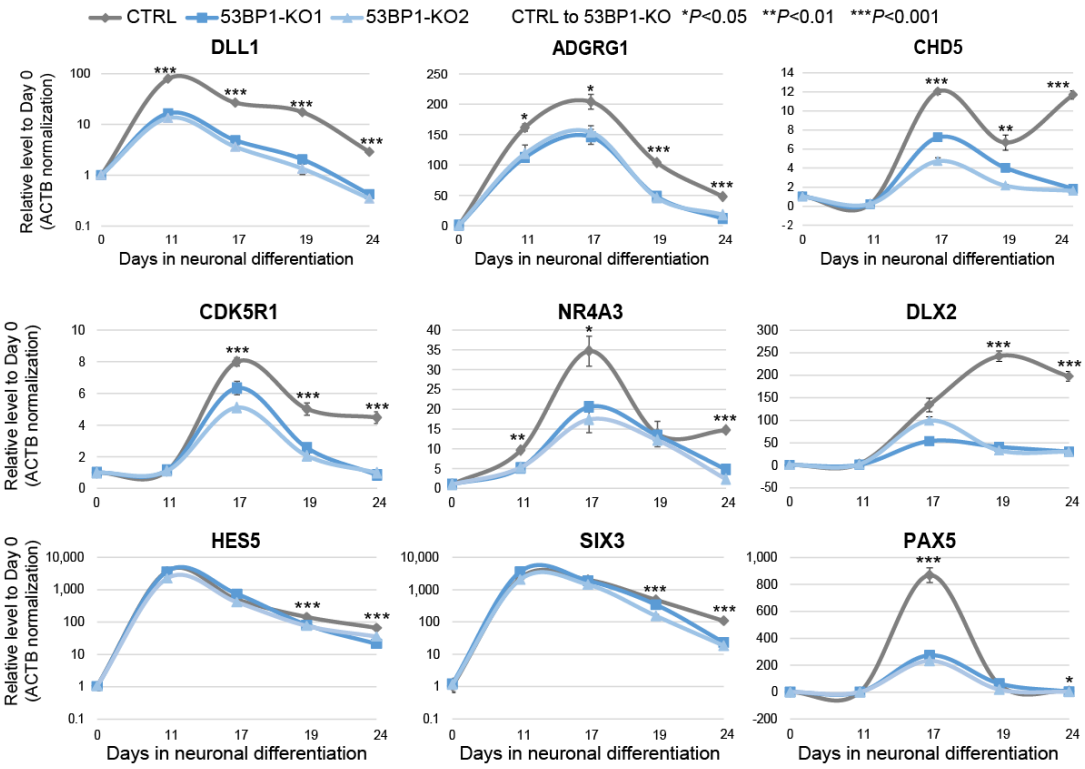

e Downregulated in both 53BP1-KO monolayer differentiation and organoids

Term	Overlap	P-value
positive regulation of synapse maturation by synaptic transmission	16/188	9.61E-10
synaptic transmission, cholinergic	16/200	2.37E-09
chemical synaptic transmission	15/180	4.35E-09
positive regulation of axon extension involved in axon guidance	6/25	3.91E-07
neurogenesis	14/272	5.11E-06
central nervous system neuron axonogenesis	7/65	1.20E-05
ganglion development	12/244	3.81E-05
autonomic nervous system development	12/245	3.96E-05
central nervous system development	14/333	4.88E-05
neural tube development	12/259	6.77E-05
determination of left/right asymmetry in nervous system	12/270	1.00E-04

Supplementary Figure 14

Gene expression profiling of control and 53BP1-KO cells during the course of neuronal differentiation.

(a) Principal component analysis of gene expression profiles of control hESCs and hNPCs at day 22 of differentiation. Dotted lines encircle different experimental groups. Numbers indicate clones; 2 sets of differentiation were performed. Gene ontology analyses of (b) downregulated and (c) upregulated expressed genes between 2 control and 3 53BP1-KO clones at day 22 of differentiation. The ontology terms were ranked by *P* value significance, with the number of bound genes indicated. (d) Transcript profiling of control cells and 2 53BP1-KO clones at days 0 (hESC state), 11, 17, 19, and 24 of differentiation. N=3 independent RT samples. Mean and standard deviation are indicated, with *, **, *** respectively indicating $P<0.05$, 0.01, or 0.001 by one-sided Student's *t*-test. (e) Gene ontology analyses of downregulated genes that are share in both 53BP1-KO monolayer differentiation (vs. control) and 53BP1-KO cortical organoids (vs. control). The ontology terms were ranked by *P* value significance, with the number of bound genes indicated. For b, c, and e, *P* values were calculated by the Fisher's exact test.

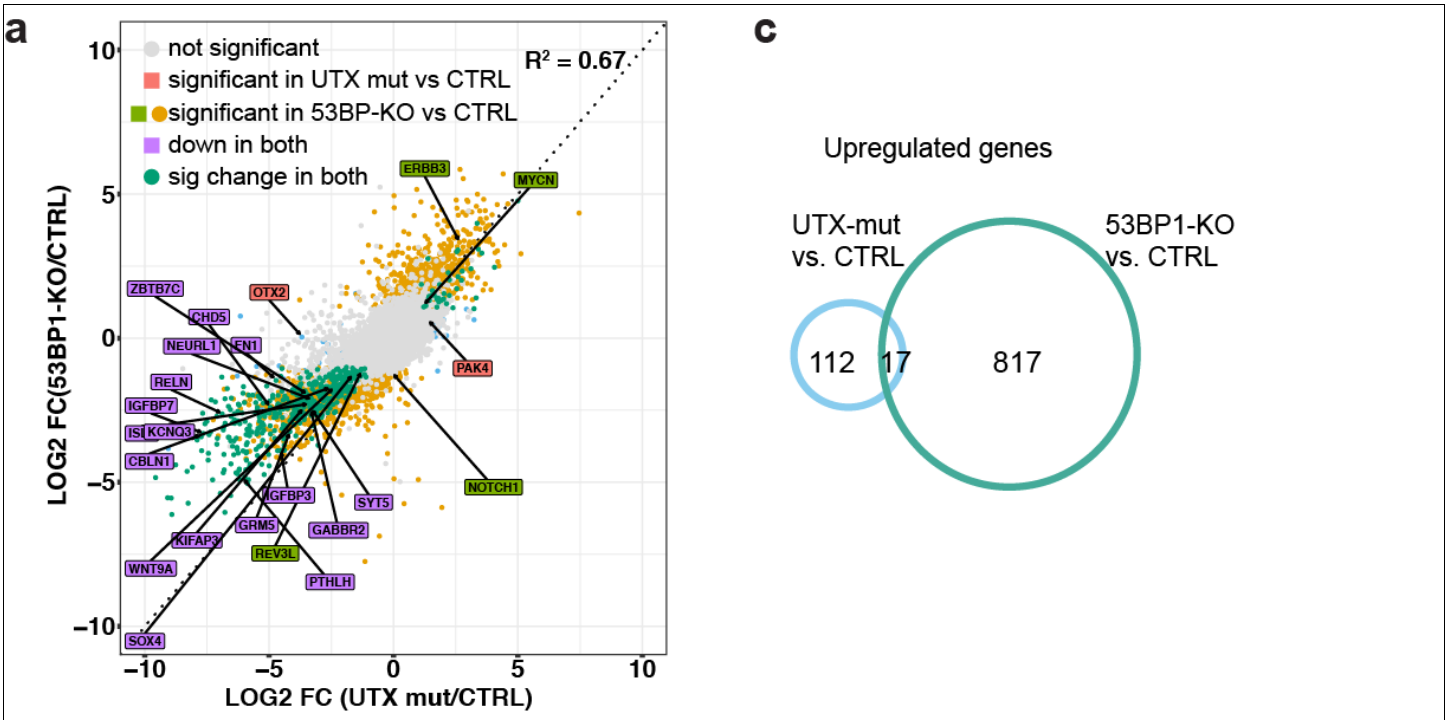

b

77 downregulated neurogenic genes in UTX mutant: ATCAY BAIAP3 CACNA1E CAMK2A CAMK2B CBLN1 CDH13 CDK5R1 COL1A1 COL4A1 CRIM1 CTNNA2 DLX2 DLX5 DLX6 DNM3 DSCAM EDN1 FGF1 FGF5 FRY GABBR2 GAD1 GAD2 GAP43 GPR149 GRM5 GRM7 HBEGF HTR2A INHBA KCNQ3 KIDINS220 KIF5A KIF5C L1CAM LAMC2 LRRC7 LY6H MAPT MPPED2 MYT1L NALCN NDRG4 NEURL1 NKX2-1 NOG NR2E1 NRSN1 NTRK1 NTRK3 OPHN1 OPRL1 PAK3 PCDHB2 PLPPR4 PNOC PTPRO RELN RIMS1 SCN1A SCN2A SCN3B SHTN1 SIX3 SLC12A5 SLC32A1 SLC4A10 SLC6A1 SLC6A17 SLITRK6 SNCAIP SPOCK2 SYT5 TMOD2 TNR UNC13C

205 downregulated neurogenic genes in 53BP1 KO: ADGRA2 ADGRL3 AKAP5 ALDH5A1 AMPH APBA1 APBA2 APBB1 APLP1 ARNT2 ASCL1 ATL1 BCL11A BCL11B BRSK2 BSN BTBD6 CACNA1E CACNB1 CACNB2 CACNB3 CAMK2A CAMK2B CBLN1 CDK5R1 CHRM5 CHRNB2 CNTN4 CNTN6 CRHBP CRIM1 CRMP1 CSPG5 CTNNA2 CYP46A1 DCC DCHS1 DCX DLL1 DLX5 DLX6 DNER DNM3 DOK6 DPF1 DPYSL2 DPYSL4 DPYSL5 DSCAM EFNB3 ENC1 EPHA5 EPHB1 EPHB2 EVL FABP7 FGF19 FGF5 FZD1 GABBR2 GABRA1 GABRG2 GAD1 GAD2 GAP43 GFRA1 GLRA2 GLRB GPC1 GPM6A GPR1 GPR149 GPR88 GRIA1 GRIA2 GRIK1 GRIK2 GRM1 GRM5 GRM7 HAPLN1 HCRTR2 HES5 HPCAL4 HTR2A IL1RAPL2 INHBA JAG1 KALRN KCNA1 KCNK3 KCNMB1 KCNQ3 KIF3A KIF3B KIF5A KIF5C KIRREL3 L1CAM LRRC55 LY6H MAB21L2 MBNL1 MCHR1 MEF2C MPPED2 MYT1L NCAM1 NCAN NDN NDP NELL1 NES NEURL1 NFASC NHLH2 NLGN3 NOG NOTCH1 NOVA1 NPAS4 NR2E1 NRCAM NRG1 NRP1 NRSN1 NRXN1 NRXN2 NRXN3 NTN1 OPHN1 OPRL1 PAK3 PAX6 PCDH17 PCDH19 PCDHA10 PCDHA11 PCDHA6 PCDHA7 PCDHA9 PCDHB10 PCDHB11 PCDHB12 PCDHB13 PCDHB14 PCDHB16 PCDHB2 PCDHB3 PCDHB4 PCDHB6 PCDHB7 PCDHB8 PCDHB9 PCDHGB6 PCDHGC4 PCDHGC5 PDE7B PDGFC PLPPR4 PMP22 PNOC POU3F3 PTPRO RBFOX1 RCAN1 RELN RNF103 ROBO2 S100A6 SCRG1 SEMA3C SEMA5A SHC3 SHTN1 SIM1 SLC12A5 SLC1A2 SLC1A4 SLC4A10 SLC6A1 SLIT1 SLIT2 SLITRK1 SLITRK3 SLITRK6 SMPD1 SNAI2 SNAP25 SOX8 SPOCK1 SPOCK2 SPTBN5 SRRM4 ST8SIA2 STMN3 SYT1 SYT5 TAGLN3 TMOD2 TNR TRIM3 TUBB3 UNC13C WNT7A

Supplementary Figure 15

Compared to control cells, UTX-KD and 53BP1-KO hNPCs share downregulated genes that are enriched in terms related to neurogenesis.

(a) Comparison of gene expression profiles of 3 (biologically independent samples) UTX-KD vs. 2 control and 3 53BP1-KO vs. 2 control by counts per million of sequencing reads for each annotated gene. The correlation coefficient between the 2 datasets is 0.67, calculated by using linear model of Goodness-of-Fit package in R. Color-coded points indicate notable genes with functions related to nervous system development. (b) Lists of 77 and 205 downregulated neurogenic genes in UTX-KD and 53BP1-KO hNPCs, respectively. (c) Venn diagram showing the overlap of upregulated genes among UTX mutant, 53BP1-KO, and control cells.

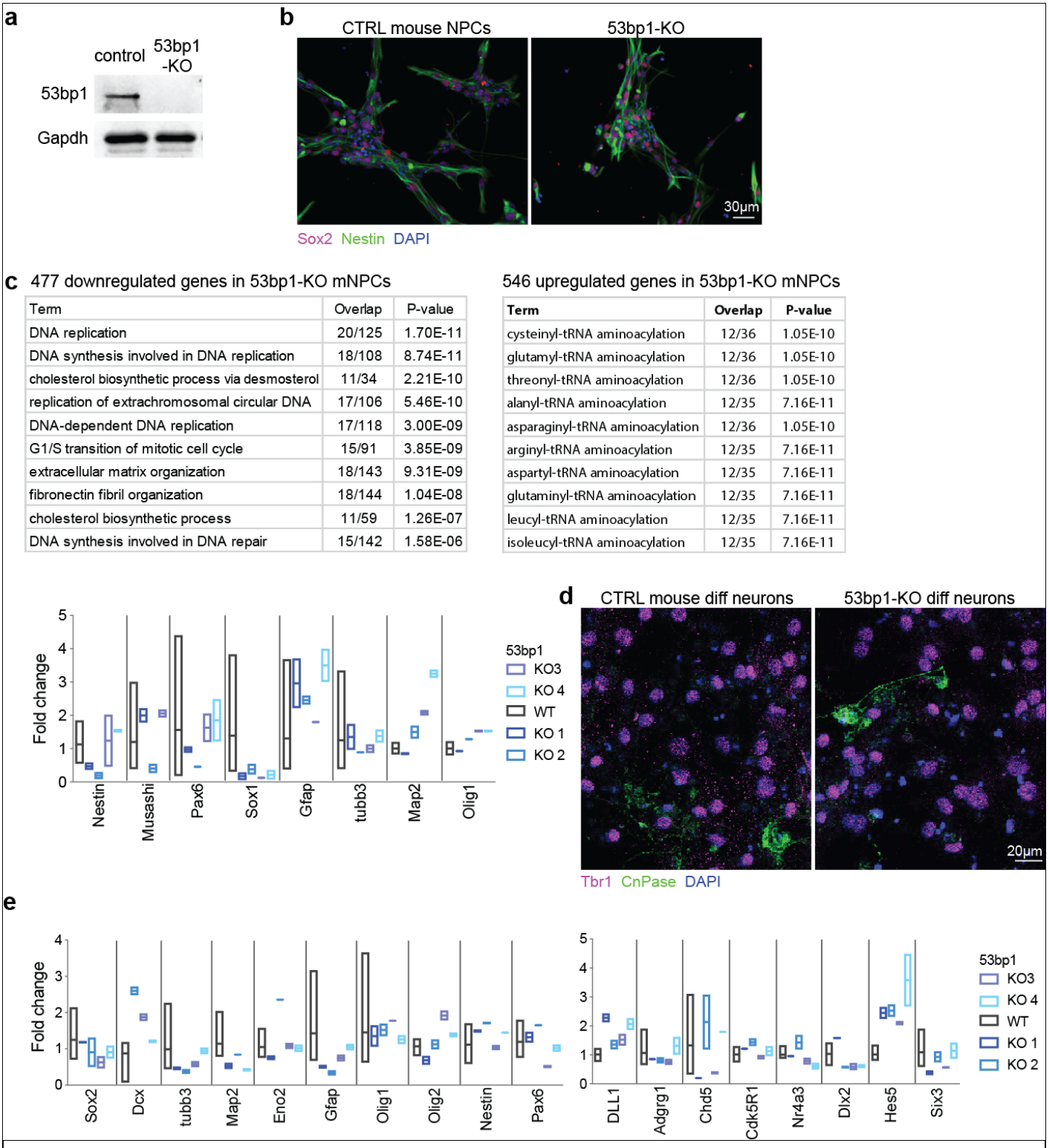

Term	Overlap	P-value
DNA replication	20/125	1.70E-11
DNA synthesis involved in DNA replication	18/108	8.74E-11
cholesterol biosynthetic process via desmosterol	11/34	2.21E-10
replication of extrachromosomal circular DNA	17/106	5.46E-10
DNA-dependent DNA replication	17/118	3.00E-09
G1/S transition of mitotic cell cycle	15/91	3.85E-09
extracellular matrix organization	18/143	9.31E-09
fibronectin fibril organization	18/144	1.04E-08
cholesterol biosynthetic process	11/59	1.26E-07
DNA synthesis involved in DNA repair	15/142	1.58E-06

Term	Overlap	P-value
cysteinyl-tRNA aminoacylation	12/36	1.05E-10
glutamyl-tRNA aminoacylation	12/36	1.05E-10
threonyl-tRNA aminoacylation	12/36	1.05E-10
alanyl-tRNA aminoacylation	12/35	7.16E-11
asparaginyl-tRNA aminoacylation	12/36	1.05E-10
arginyl-tRNA aminoacylation	12/35	7.16E-11
aspartyl-tRNA aminoacylation	12/35	7.16E-11
glutaminyl-tRNA aminoacylation	12/35	7.16E-11
leucyl-tRNA aminoacylation	12/35	7.16E-11
isoleucyl-tRNA aminoacylation	12/35	7.16E-11

Supplementary Figure 16

Murine 53bp1 does not impact mNPCs. (a) WB analysis of control and 53bp1-KO mNPCs.

(b) IF of Sox2 and Nestin in control and 53bp1-KO mNPCs. Bar, 30µm. (c) Gene ontology analysis of differentially expressed genes between RNA-seq datasets from 4 control and 4 53bp1-KO mNPCs. RT-qPCR profiling of key neurodevelopmental genes, with n=3 biological RT samples and no difference by the ANOVA test. Mean and standard deviation are indicated. (d) IF of Tbr1 and CnPase in control and 53bp1-KO mNPCs at day 21 of differentiation. Bar, 30µm. (e) Transcript profiling by RT-qPCR of control and 53bp1-KO cells at day 21 of differentiation. The assayed genes are key neurodevelopmental genes and those perturbed by 53BP1 KO in hNPCs. Mean and standard deviation are indicated. Control are sibling heterozygous 53bp1 -/+ mNPCs. N=3 biological RT samples. No significant differences observed between control and 53bp1-KOs by the ANOVA test. Experiments were repeated 3 times for a and b and 2 times for d to yield similar results. WB images are cropped.

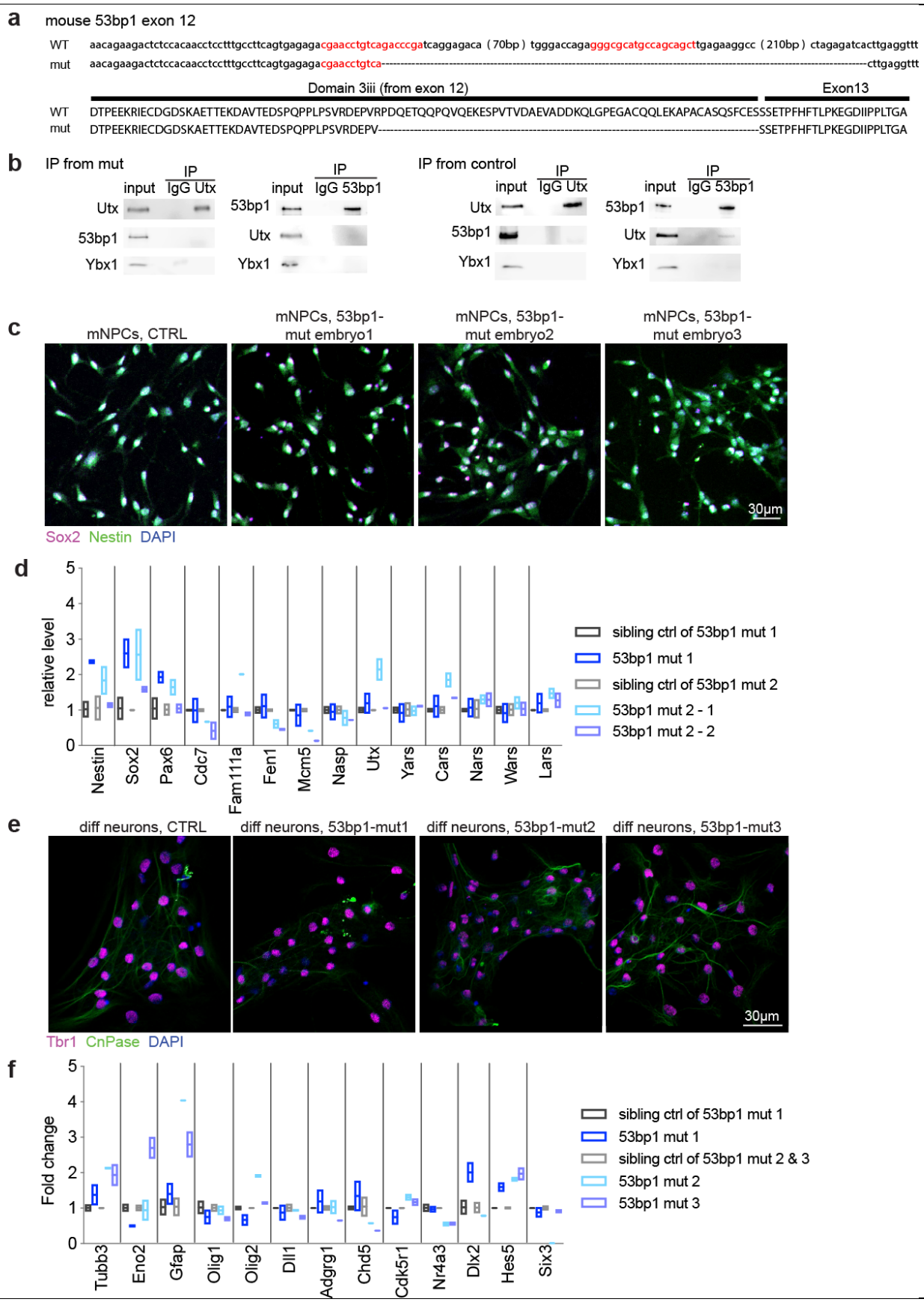
a
mouse 53bp1 exon 12
WT aacagaagactctccacaacctcctttgccttcagtgagagacgaacctgtcagacccgatcaggagaca (70bp) tgggaccagagggcgcatgccagcagcttgagaaggcc (210bp) ctagagatcacttgaggttt
mut aacagaagactctccacaacctcctttgccttcagtgagagacgaacctgtca----------cttgaggttt
Domain 3iii (from exon 12)
Exon13
WT DTPEEKRIECDGDSKAETTEKDAVTEDSPQPPLPSVRDEPVRPDQETQQPQVQEKESPVTVDAEVADDKQLGPEGACQQLEKAPACASQSFCESSSETPFHFTLPKEGDIIPPLTGA
mut DTPEEKRIECDGDSKAETTEKDAVTEDSPQPPLPSVRDEPV----------SSETPFHFTLPKEGDIIPPLTGA
b
IP from mut
input
IP
IgG Utx
IgG 53bp1
Utx
53bp1
Ybx1
IP from control
c
mNPCs, CTRL
mNPCs, 53bp1-mut embryo1
mNPCs, 53bp1-mut embryo2
mNPCs, 53bp1-mut embryo3
30μm
Sox2 Nestin DAPI
d
relative level
Nestin
Sox2
Pax6
Cdc7
Fam111a
Fen1
Mcm5
Nasp
Utx
Yars
Cars
Nars
Wars
Lars
sibling ctrl of 53bp1 mut 1
53bp1 mut 1
sibling ctrl of 53bp1 mut 2
53bp1 mut 2 - 1
53bp1 mut 2 - 2
e
diff neurons, CTRL
diff neurons, 53bp1-mut1
diff neurons, 53bp1-mut2
diff neurons, 53bp1-mut3
30μm
Tbr1 CnPase DAPI
f
Fold change
Tubb3
Eno2
Gfap
Olig1
Olig2
Dll1
Adgrg1
Chd5
Cdk5r1
Nr4a3
Dlx2
Hes5
Six3
sibling ctrl of 53bp1 mut 1
53bp1 mut 1
sibling ctrl of 53bp1 mut 2 & 3
53bp1 mut 2
53bp1 mut 3

Supplementary Figure 17

Disruption to Utx-53bp1 binding does not impact mNPCs.

(a) CRISPR (red) sequences and mutation in the murine 53bp1 gene locus. Amino acids within domain 3iii of the mouse 53bp1. Dots indicate deletions. (b) WB analysis of IP from 53bp1 mutant and control embryos. (c) IF of Sox2 and Nestin in control and 53bp1 mutant mNPCs. Bar, 30μm. (d) Transcript profiling of control and 53bp1 mutant mNPCs. The assayed genes are key neurodevelopmental genes and those perturbed by 53bp1 KO in mNPCs. N=3 biological RT samples and no difference by the ANOVA test. (e) IF of Tbr1 and CnPase in control and 53bp1 mutant cells at day 14 of differentiation. Bar, 30μm. (f) Transcript profiling of control and 53bp1-KO cells at day 21 of differentiation. The assayed genes are key neurodevelopmental genes and those perturbed by 53BP1 KO in hNPCs. Mean and standard deviation are indicated. N=3 biological RT samples. No significant differences were observed between 53bp1 mutant and control groups by the ANOVA test. 53bp1 mutant 1 came from a genetic cross / mother separate from that of mutants 2 and 3. Experiments were repeated 2 times for b, c, and e to yield similar results. WB images are cropped.

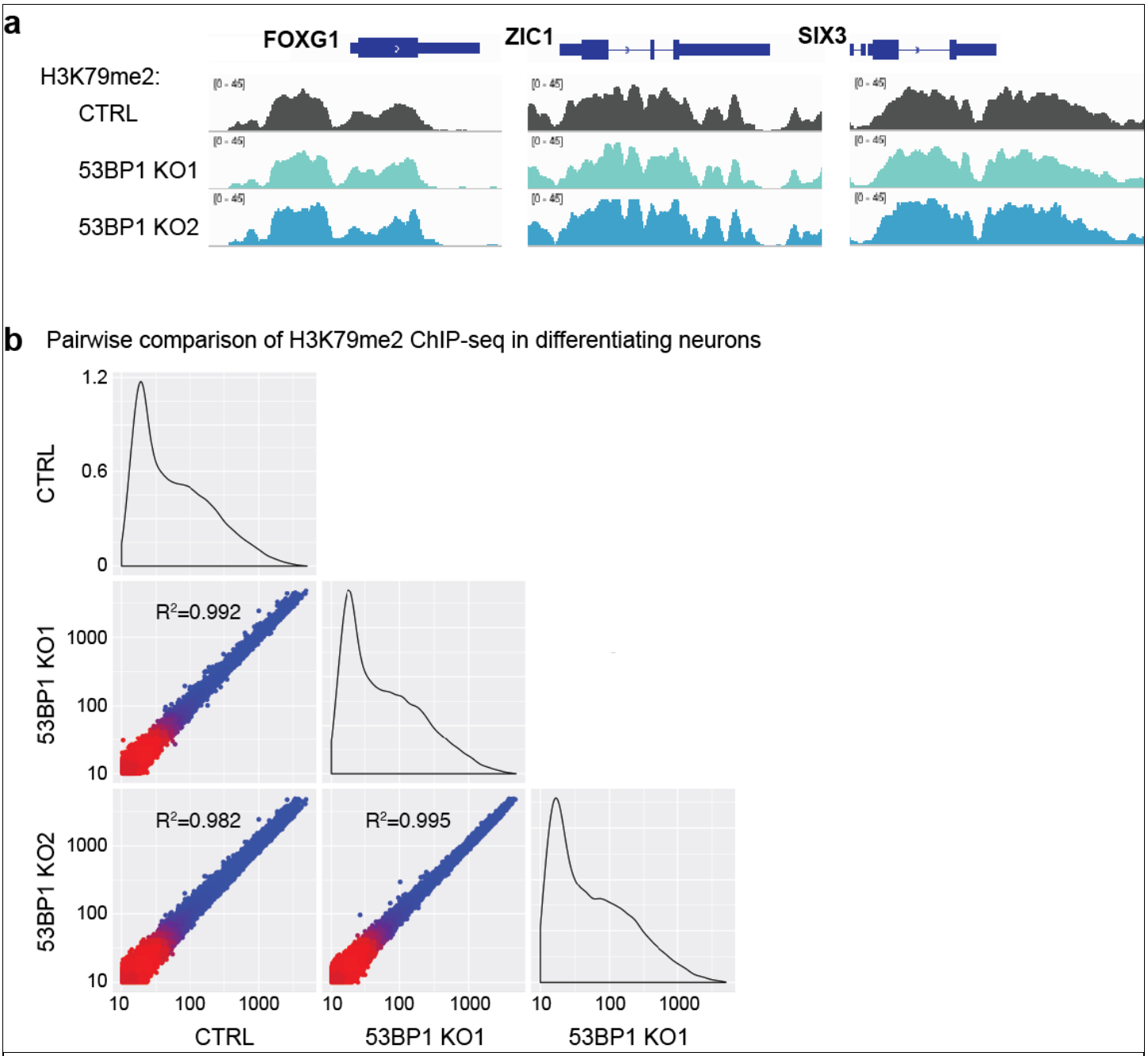

Supplementary Figure 18

53BP1 does not affect H3K79me2 localization in hESCs.

(a) Representative H3K79me2 ChIPseq tracks at neurogenic genes in control and 53BP1-KO hNPCs at day 17 of differentiation. Experiments were repeated 2 times to yield similar results. (b) High correlation between H3K79me2 ChIP-seq datasets from control and 53BP1-KO hNPCs at day 17 of differentiation. R^2 values are Pearson correlation coefficients. 1 control and 2 independent 53BP1-KO samples were analyzed.

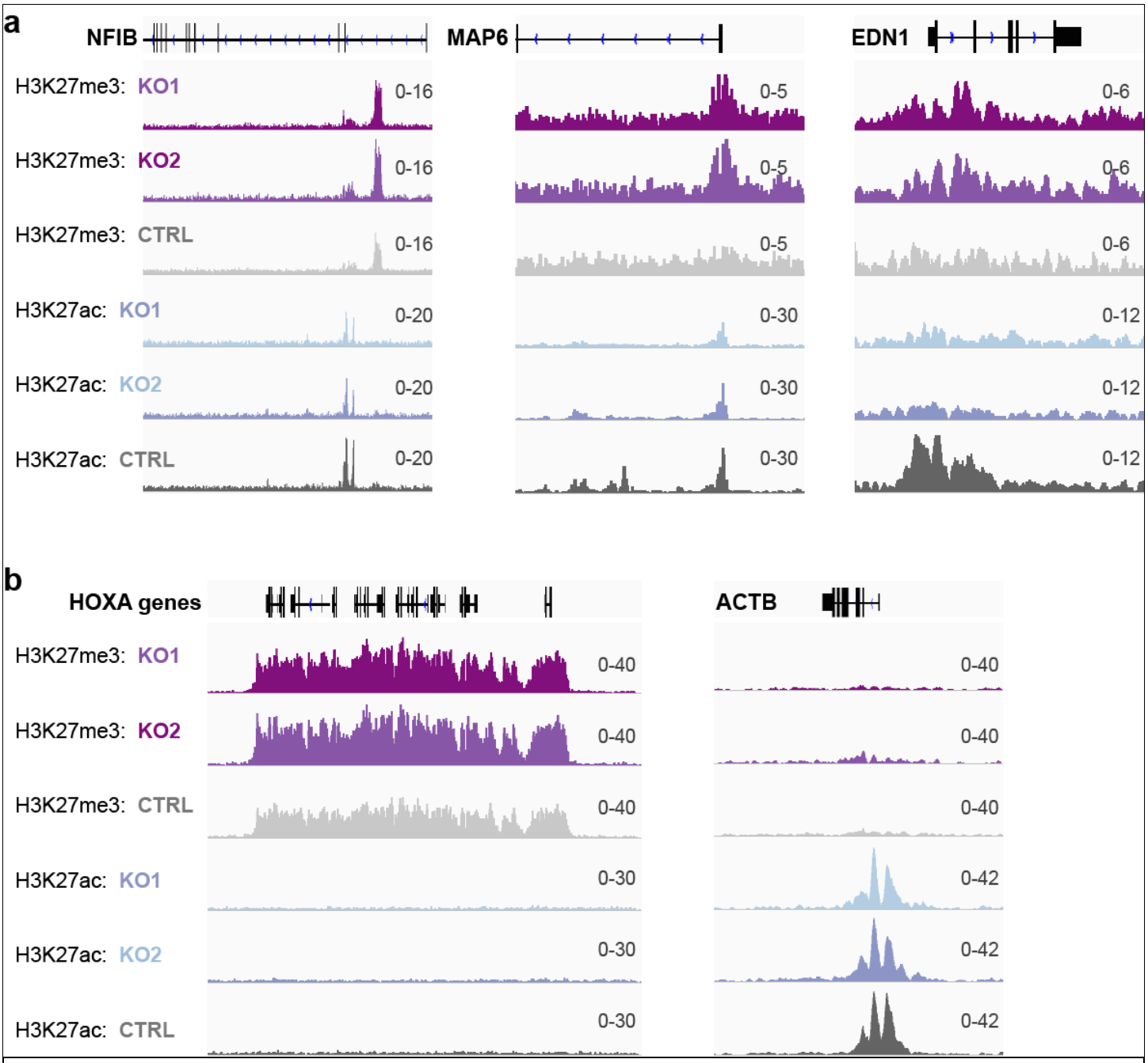

Supplementary Figure 19

Histone H3K27me3 and H3K27ac ChIP-seq tracks at different loci of control and 53BP1-KO cells at day 22 of neuronal differentiation.

In contrast to Fig 6, the ChIPseq tracks in control cells are displayed separately from those in 53BP1-KO cells. (a) The NFIB, MAP6, and EDN1 genes were downregulated in 53BP1-KO hNPCs and associated with significantly higher H3K27me3 but significantly lower H3K27ac. (b) Genes in the HOXA cluster were silenced and associated with high H3K27me3 level but non-detectable H3K27ac. The ACTB gene was expressed and associated with non-detectable H3K27me3 level and high H3K27ac. Experiments were repeated 2 times to yield similar results.

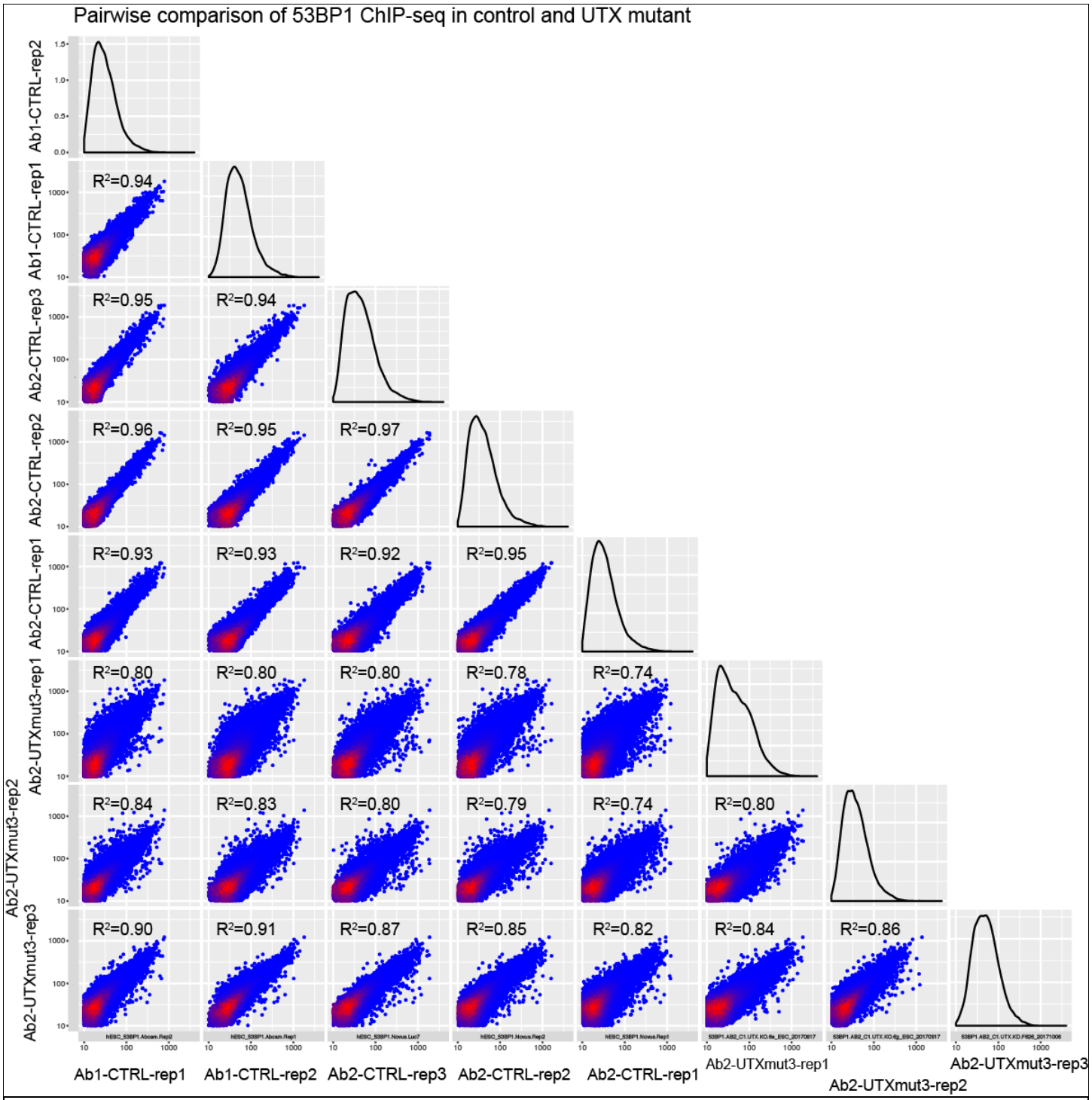

Supplementary Figure 20

53BP1 genome-wide bindings change between control and UTX mutant differentiating neurons.

Each dataset is ChIP-seq signals at binned genomic regions. Pairwise counts per million of the datasets, with respective R^2 values, which are Pearson correlation coefficients. Red indicates a higher density of points. Diagonal curve plots show the kernel density of ChIP-seq reads in each dataset. 3 biologically independent 53BP1 ChIP with UTX-depleted and 5 biologically independent 53BP1 ChIP with control samples were analyzed.

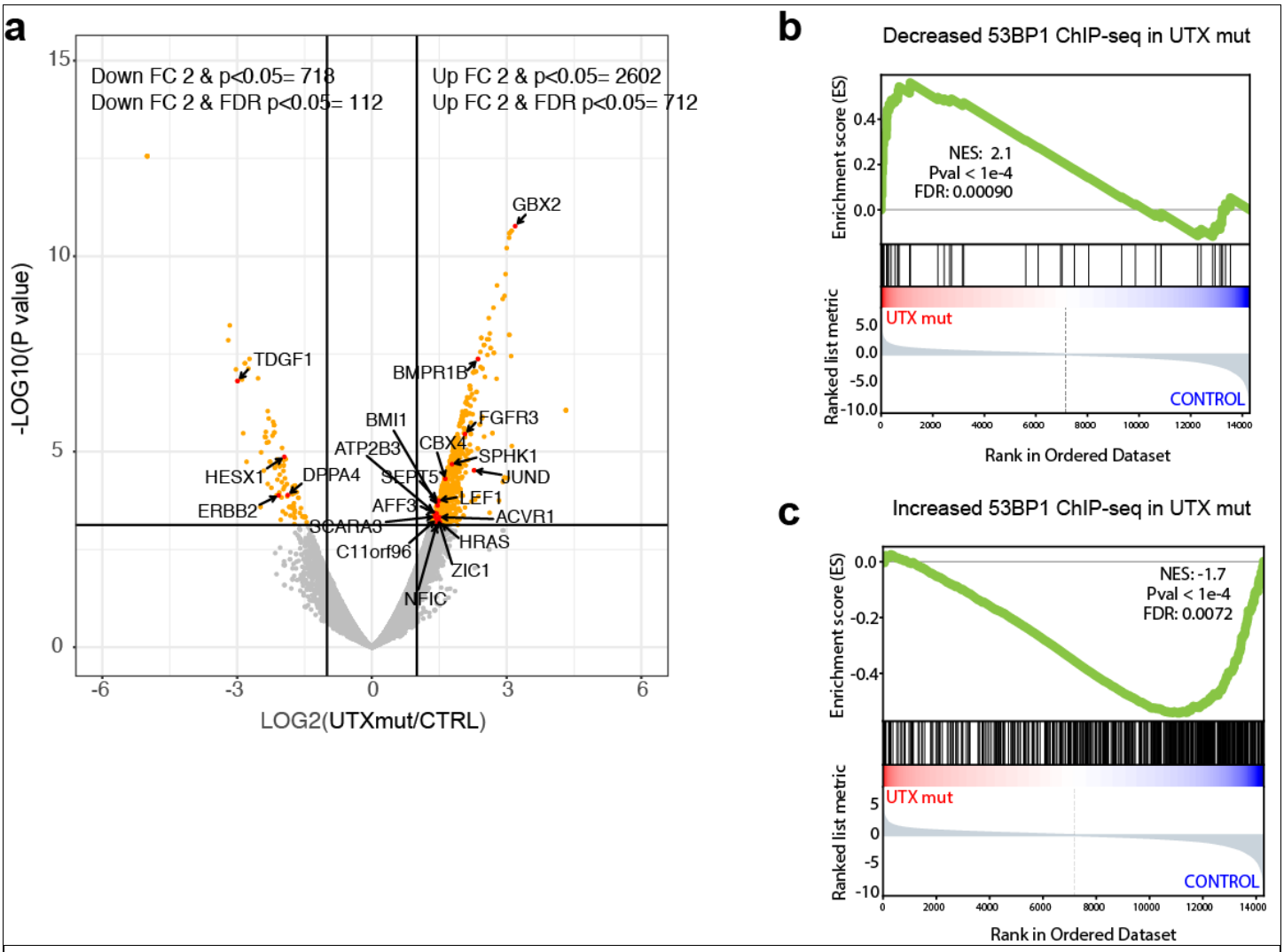

Supplementary Figure 21

UTX positively and negatively regulates 53BP1 binding to chromatin.

(a) Volcano plot of 53BP1 ChIP-seq signals in UTX mutant / control differentiating neurons. Analysis was done with modified t test in the voom package of R. Notable development-relevant genes are noted. Gene set enrichment analysis of (b) genes having decreased 53BP1 binding or (c) genes having increased 53BP1 binding with differentially expressed genes in UTX mutant vs. control differentiating neurons. For a-c, 3 biologically independent 53BP1 ChIP with UTX-depleted and 5 biologically independent 53BP1 ChIP with control samples were analyzed.

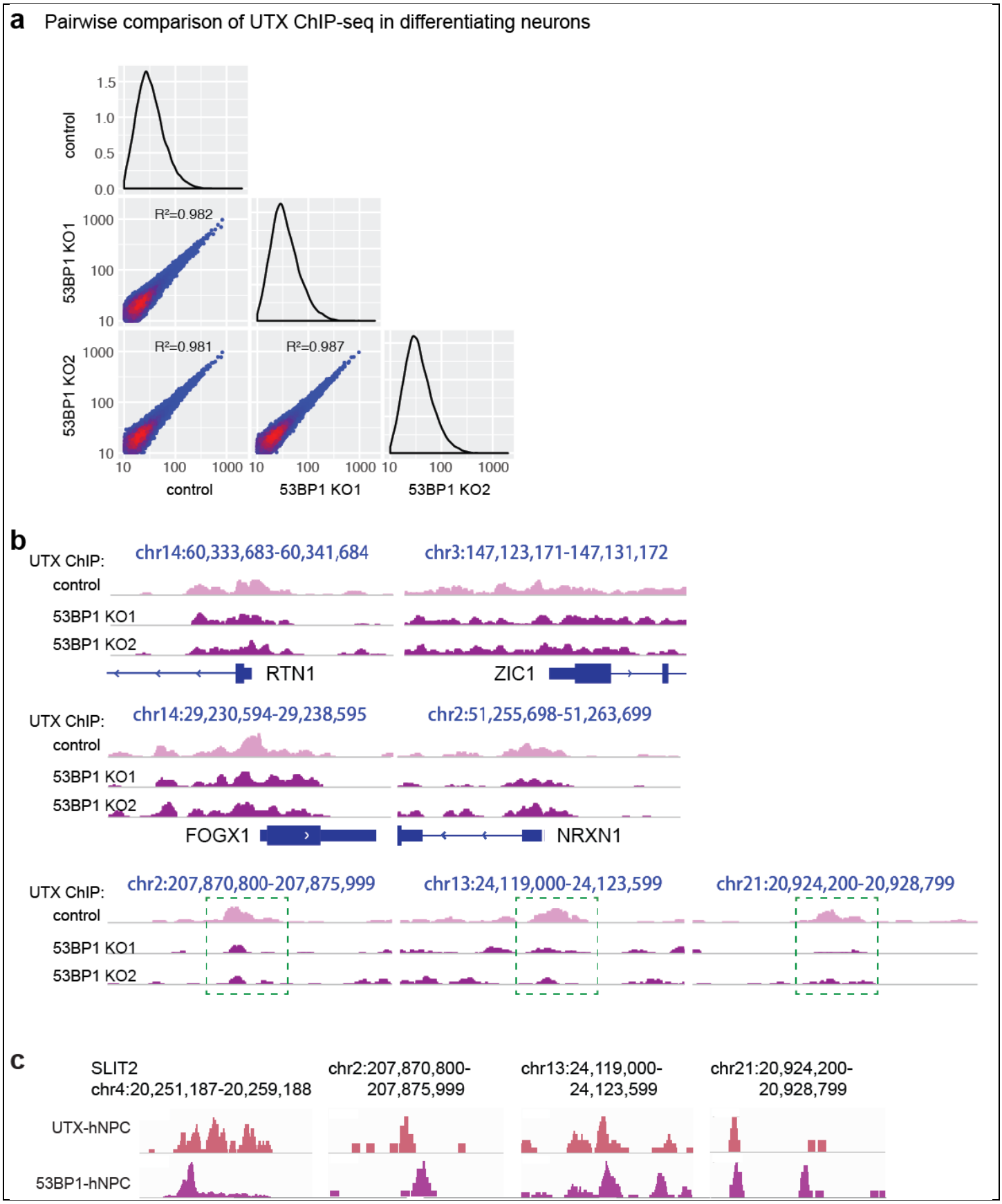
a
Pairwise comparison of UTX ChIP-seq in differentiating neurons
control
53BP1 KO1
53BP1 KO2
R²=0.982
R²=0.981
R²=0.987
b
UTX ChIP:
chr14:60,333,683-60,341,684
chr3:147,123,171-147,131,172
RTN1
ZIC1
chr14:29,230,594-29,238,595
chr2:51,255,698-51,263,699
FOGX1
NRXN1
chr2:207,870,800-207,875,999
chr13:24,119,000-24,123,599
chr21:20,924,200-20,928,799
c
SLIT2
chr4:20,251,187-20,259,188
UTX-hNPC
53BP1-hNPC

Supplementary Figure 22

53BP1 affects UTX binding to select gene targets.

(a) Pairwise comparison of UTX ChIP-seq datasets at binned genomic regions in control and 53BP1-KO at day 17 of differentiation. Pairwise counts per million of the datasets, with respective R^2 values, which are Pearson correlation coefficients. Red indicates a higher density of points. Diagonal curve plots show the kernel density of ChIP-seq reads in each dataset. 2 biological samples were analyzed. (b) UTX ChIPseq tracks at neurogenic genes and gene targets with changed UTX binding in control and 53BP1-KO hNPCs at day 17 of differentiation. Dotted green boxes indicate sites with lower UTX levels. (c) UTX and 53BP1 ChIPseq tracks at different sites in control hNPCs at day 15 of differentiation. Experiments were repeated 2 times to yield similar results.

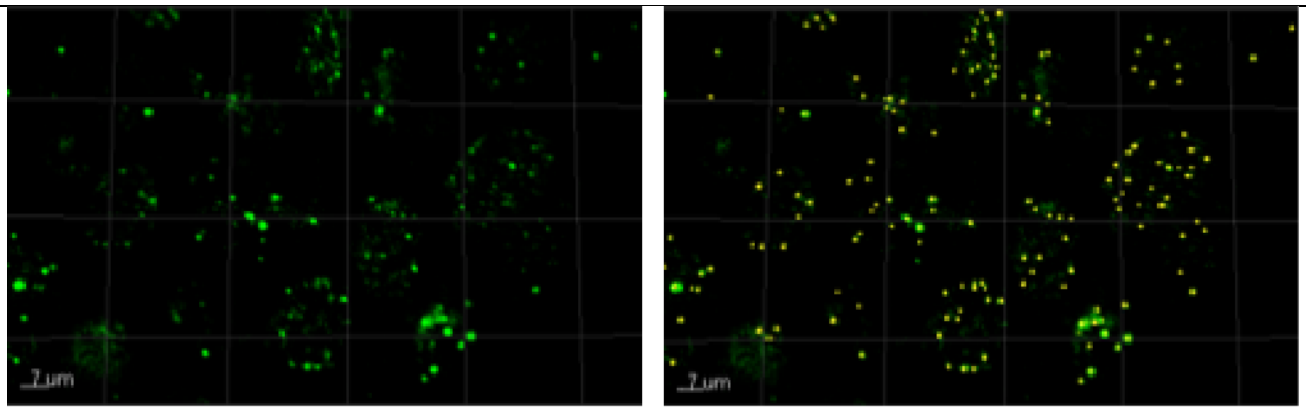

Supplementary Figure 23

Examples of image processing by Imaris to identify double-stranded breaks.

Left image is **γ**H2AX (green) immunofluorescence of control H9 hESCs. Right is a processed image by using the Imaris 8.4 to threshold IF signals and identify double-stranded breaks (yellow-pseudocolored).